
SCUOLA DI SCIENZE

Dipartimento di Chimica Industriale “Toso Montanari”

Corso di Laurea Magistrale in

Chimica Industriale

Classe LM-71 - Scienze e Tecnologie della Chimica Industriale

Towards the Kinetic Resolution of Mechanically Planar Chiral Rotaxanes

Tesi di laurea sperimentale

CANDIDATO

Alessandro Turci

RELATORE

Dr. Stefano Corrà

CORRELATORE

Dr. Federico Nicoli

Anno Accademico 2021-2022

ABSTRACT

In this work, we reported the synthesis and characterization of two [2]rotaxanes endowed with a central ammonium group and two triazolium recognition stations on either side, acting as complexation sites for a dibenzo-24-crown-8 ether macrocycle. These mechanically interlocked architectures were obtained through the interlocking of a functionalized achiral macrocycle with C_s symmetry (where the symmetry element is a mirror plane corresponding to plane of the ring) and a $C_{\infty v}$ symmetric axle (where a mirror plane and a C_{∞} principal axis are aligned along the axle length).

We took advantage of the reversible acid/base triggered molecular shuttling of the ring between two lateral triazolium units to switch the rotaxanes between prochiral and mechanically planar chiral forms, which exists as two rapidly-interconverting co-conformers.

We exploited the reactivity of the central amino group to attach an optically pure chiral substituent, with the goal of demonstrating the enantiomeric nature of the co-conformers and to obtain a non-zero diastereomeric excess in the resulting diastereomeric products through a dynamic kinetic resolution. To this end, two enantiopure reagents were chosen that could perform clean and fast reaction with amines: a sulfonyl chloride and an acyl chloride. Only the acyl chloride successfully produced an amide in high yield with the deprotonated rotaxane. The group added to the central amine station acted as a stopper against the shuttling of the macrocycle along the axis, thus preventing the fast interconversion of the two mechanically planar enantiomers.

We analysed the results through static and dynamic NMR spectroscopic techniques by varying temperature and solvent used. Indeed, the presence of diastereomers was recorded alongside the configurational isomers resulting from the slow rotation of the CN-CO bond of the amide moiety, thus paving the way for a dynamic kinetic resolution.

RIASSUNTO

In questo lavoro, è riportata la sintesi e la caratterizzazione di due [2]rotassani dotati di un gruppo ammonio centrale e due stazioni di riconoscimento triazolico laterali, che si comportano come siti di complessazione per un macrociclo dibenzo-24-corona-8 etere. Queste architetture meccanicamente interconnesse sono state ottenute attraverso la concatenazione di un macrociclo funzionalizzato di simmetria C_s (dove l'elemento di simmetria è un piano di riflessione corrispondente al piano dell'anello) ed un asse di simmetria $C_{\infty v}$ (dove un piano di riflessione e un asse di rotazione C_{∞} sono allineati lungo la lunghezza dell'asse stesso).

Il moto di traslazione dell'anello tra le due stazioni triazolico, indotto da reazioni acido/base, converte i rotassani dalla loro forma prochirale alla forma chirale meccanico-planare, la quale esiste sottoforma di due co-conformer in rapida interconversione.

La reattività del gruppo amminico centrale è stata sfruttata per attaccare un sostituito chirale otticamente puro, con l'obiettivo di dimostrare la natura enantiomerica dei co-conformer e di ottenere un eccesso diastereoisomerico nei prodotti attraverso una risoluzione cinetica dinamica. A tal fine, due reagenti enantiopuri sono stati scelti affinché reagissero con l'ammina in maniera pulita e veloce: un sulfonil cloruro e un acil cloruro. Solo l'acil cloruro è riuscito a produrre un'ammina in alta resa con il rotassano deprotonato. Il gruppo aggiunto alla stazione amminica centrale si è comportato come un ostacolo al moto di scorrimento del macrociclo lungo l'asse, impedendo la veloce interconversione tra i due enantiomeri meccanico-planari.

Abbiamo analizzato i risultati attraverso spettroscopia NMR sia statica che dinamica, variando la temperatura e il solvente utilizzati. Infatti, la presenza di diastereoisomeri è stata osservata assieme a quella degli isomeri configurazionali provenienti dalla rotazione lenta del legame CN-CO del gruppo funzionale ammidico, aprendo la strada per una risoluzione cinetica dinamica.

TABLE OF CONTENTS

1. INTRODUCTION.....	9
1.1 Mechanical Bond and Mechanically Interlocked Molecules (MIMs)	9
1.2 Ring Shuttling and Switching	13
1.3 Chirality.....	16
1.4 Mechanically Planar Chirality.....	18
1.5 On-off switching of chirality.....	19
1.6 Kinetic Resolution.....	21
2. AIM OF THE THESIS.....	25
3. RESULTS AND DISCUSSION	27
3.1 Synthesis and purification of the asymmetric [2]rotaxanes	27
3.2 Synthesis of the axle precursor.....	28
3.3 Synthesis of the “oriented” crown ethers	29
3.4 Synthesis of prochiral rotaxanes 1a and 1b.....	31
3.5 Acid/base-induced ring shuttling	34
3.6 Kinetic resolution	37
3.7 Reaction with camphorsulfonyl chloride	38
3.8 Reaction with camphanyl chloride.....	41
4. CONCLUSIONS.....	49
5. EXPERIMENTAL SECTION	51
5.1 Synthesis of the oriented crown ethers.....	52
5.2 Synthesis of the asymmetric rotaxanes	57
6. REFERENCES.....	67

1. INTRODUCTION

1.1 Mechanical Bond and Mechanically Interlocked Molecules (MIMs)

Two or more distinct molecules can be defined as “mechanically interlocked” when they cannot be separated without breaking a covalent bond. The nature of their entanglement is, therefore, that of a physical – more than chemical – bond, and we refer to it as “mechanical bond”.¹ Molecular structures displaying at least one mechanical bond are called “mechanically interlocked molecules” (MIMs).

It is noteworthy that, while chemical bonds owe their existence to attractive forces between single atoms, the mechanical bond relies in fact on repulsive forces between whole molecular components that prevent them from intersecting, similarly to what happens in the macroscopic world for knots and links. Consequently, the components of the MIMs cannot be separated without breaking a covalent bond.¹

The two archetypal examples of MIMs are the catenanes and the rotaxanes. Catenanes are molecules which comprise two, or more, linked macrocyclic components, analogously to the links of a chain. Rotaxanes, on the other hand, are composed of at least one linear, dumbbell shaped, component (the “axle”) threaded through at least one macrocycle (the “ring”).¹ Their macroscopic analogous could be seen in the washer kept between a nut and a bolt.

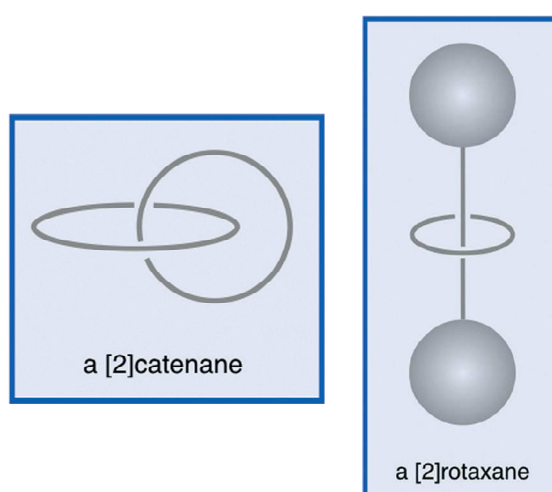


Figure 1. schematic representation of a catenane (left) and a rotaxane (right). The number in square brackets represents the number of components.

While catenanes display a complex topology – the two rings cannot even theoretically be separated without breaking at least one of them, rotaxanes are topologically trivial entities.² In rotaxanes, in fact, disentanglement of the ring component is prevented by the presence of two bulky groups, called “stoppers” at the two ends of the axle. These stoppers need to be bulky enough to mechanically block the slippage of the ring over them, or, in other words, the activation energy for the slippage process must be high. Therefore, we can define rotaxanes as “kinetically trapped” structures.³

These, relatively exotic, classes of molecules were first prepared by Wasserman in a landmark paper in the 1960s. In that pioneering work a statistical approach was exploited, which resulted in extremely small yields of the interlocked architectures.⁴

Several approaches were developed over the last 50 years for the efficient synthesis of rotaxanes. The breakthrough step in the synthesis of mechanically interlocked molecules, in fact, relies on the preorganization of the components, that is the control over the spatial organization of the molecules prior reaction. This can be achieved exploiting *self-assembly* of the components and the use of templates.⁵ The use of self-assembly for preorganizing the components in order to achieve mechanically interlocked architectures was investigated for the first time by Sauvage, basing on the work of Lehn. The strategy developed is called *passive metal templated synthesis*, where a Cu(I) ion is used as a “glue” to hold together, in a tetrahedral metal complex, the unclipped precursors of the catenane in the optimal position and orientation.⁶ Subsequently a ring closing reaction (*clipping*) is performed on the preformed complex which closes the link. Noteworthy, upon removal of the metal ion the two distinct macrocycles remain linked together as a catenane.

This strategy is also called *clipping* and involves the closure of the ring around an already formed dumbbell-shaped axle, or macrocycle. Due to topological reasons, it is the only strategy applicable to the preparation of catenanes.

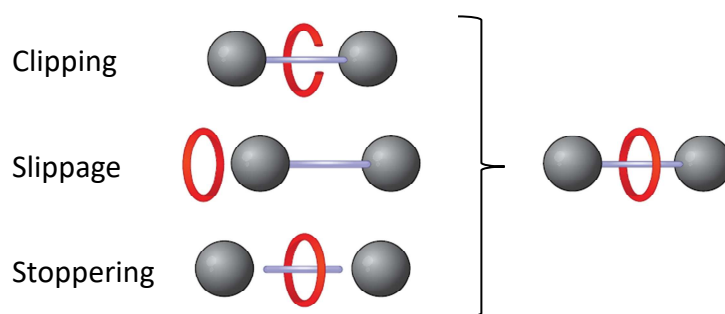


Figure 2. methods of synthesis of rotaxanes. “Clipping” (top) involves the ring closure around the already formed axle; “Slippage” (middle) sees the macrocycle overcoming the energy barrier of the stoppers due to high pressure and/or temperature; “Stoppering” (bottom) is obtained through the derivatization of a pseudo-rotaxane’s extremities with bulky groups.

On the other hand, rotaxane a topologically trivial, therefore, *slippage* of a macrocycle on a preformed dumbbell-shaped axle is a feasible method provided which solely relies on self-assembly and on a finely-tuned structure of both the axle and the ring. The macrocycle can overcome the energy barrier, namely the stoppers, for the formation of a thermodynamic stable complex with the axle only if enough energy is applied, in the form of temperature and pressure.⁷

Among the templated strategies for the preparation of rotaxanes, *stoppering* was the first developed and remains the among the most common to this day. In this method, self-assembly is exploited to thread an axle into a macrocycle, forming a supramolecular or a coordination complex called *pseudo-rotaxane*. This bears all features of a rotaxane in terms of interlocking of the components but lacks the stoppers, and is, thus, in equilibrium with its unthreaded components. Upon derivatization of the axle extremities with bulky groups, however, a rotaxane is obtained.³

An alternative approach was later developed by Leigh and coworkers in which the catalytic properties of the metal ion are fully exploited in an *active* metal template synthesis. In this mechanism, the macrocycle holds the metal ion in its cavity, inducing a pre-organization the components that leads to the catalytic formation of the covalent bond between the two halves of the axle *through* the ring.⁸

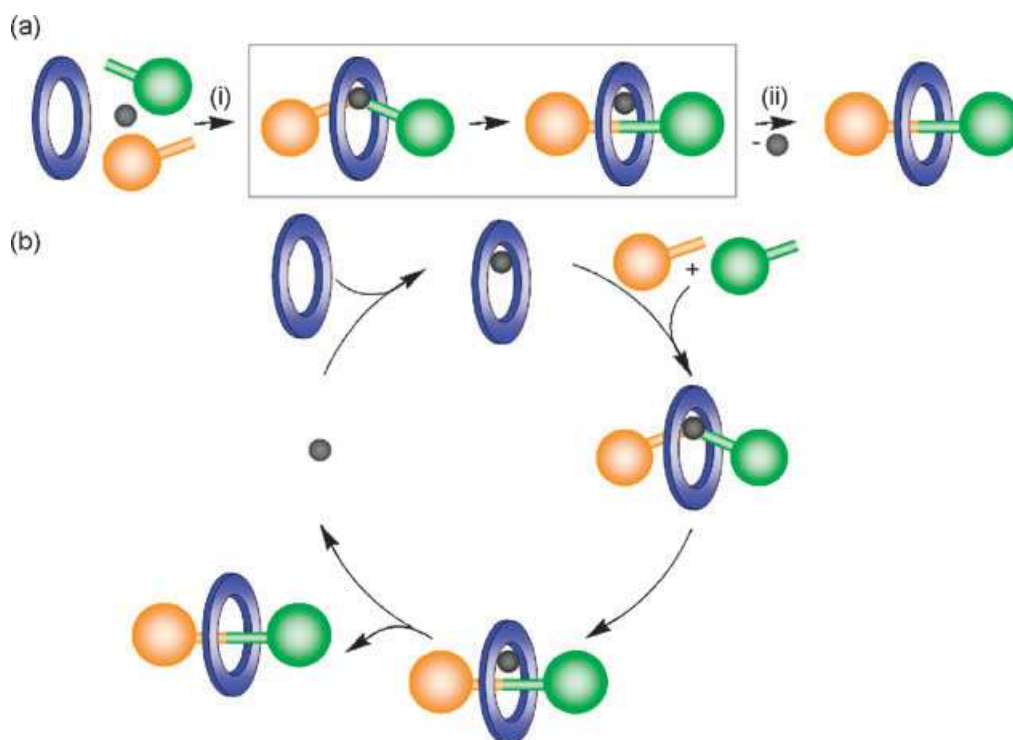


Figure 3. (a) Stoichiometric active metal template synthesis of a [2]rotaxane: (i) template assembly and covalent bond forming catalysis; (ii) subsequent demetallation. (b) Catalytic active metal template synthesis of a [2]rotaxane.

As mentioned above, however, metal ions are not the only way to preorganize the components that should form a MIM. A mechanism for self-assembly that doesn't rely on metal ions was studied for the first time in 1996 by Stoddard and co-workers, and it consists on the spontaneous complexation of the crown ether with the axle.⁹ The formation of a strong hydrogen bond was detected via NMR in a 1:1 mixture of dibenzo(24)crown-8 ether (DB24C8) and di-*n*-butylammonium hexafluorophosphate. Structural analysis of the supramolecular complex revealed that the ammonium component was threaded through the macrocycle, similarly to a wheel on an axle. For this reason, the combination of ammonium ions with DB24C8-type macrocycle became a landmark strategy for rotaxane synthesis. In fact, the same group, later reported on the conversion of the starting pseudo-rotaxane into an actual [2]rotaxane.¹⁰ This was achieved by adding bulky stoppers, in the form of (triphenylphosphonium)methyl moieties, at the extremities of the ammonium axle in the supramolecular complex. The dumbbell-shaped ammonium-based axle now prevents slippage of the ring and the entangled structure can be isolated and characterized. Moreover, phosphonium functional groups render the [2]rotaxane amenable of further functionalization via Wittig reactions without affecting the mechanically interlocked architecture.

1.2 Ring Shuttling and Switching

One of the most important characteristics of the mechanically interlocked molecules is their ability to undergo controlled, large-amplitude motion between their components, at the nanoscale.¹¹

As described in the previous section, rotaxanes are MIMs constituted by a dumbbell-shaped molecule threaded through the cavity of a ring-shaped molecule. While the mechanical bond between the two components doesn't allow their dissociation, it allows instead some degree of freedom in the form of a "shuttling" movement of the ring along the axis.³

The motion can be induced by reversibly forming and breaking the noncovalent interactions between subcomponents through external stimuli. Among these stimuli, pH stimulation is one of the most common and widely used means of controlling motion by acid and bases.¹¹

Consequently, rotaxanes became a versatile platform to construct stimuli-responsive molecular shuttles by including in their architecture recognition sites characterized by different binding affinities with the ring. Mechanical movement is produced from the drastic changes in the affinity between the recognition sites and the ring obtained through protonation/deprotonation by acids and bases.¹¹

A variety of recognition sites were then developed. Among these, Coutrot and co-workers discovered the capability of N-methyltriazolium station to act as a binding site for the ring, allowing at the same time an easy method of placing multiple stations in the axle structure through a copper-catalysed azide-alkyne cycloaddition (CuAAC).¹²

The movement of the ring along the axle was observed by Stoddart in 1997 when a DB24C8 crown ether shuttled from the amine station to the bipyridinium after the ammonium deprotonation. The movement was detected using advanced tools of the NMR spectroscopy, such as NOE spectra.¹³ Rotaxanes with more complex structure and movement were synthesized by Leigh in 2012. While DB24C8 was kept as the ring component, the axle was equipped with three recognition sites instead of two: one central ammonium station and two specular triazolium stations on both sides.

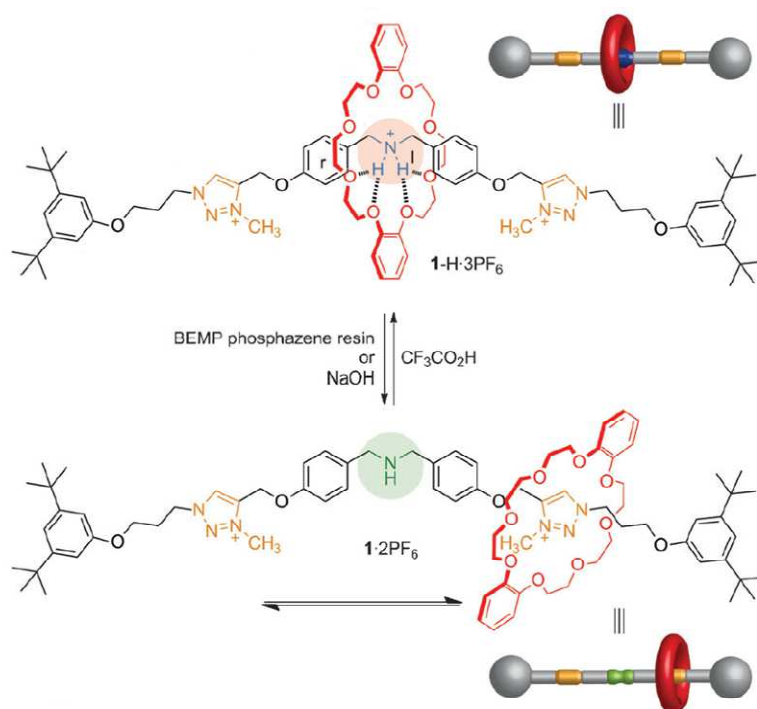


Figure 4. acid/base switching of a [2]rotaxane. The deprotonation of the ammonium station initiates the shuttling movement of the ring between the two triazolium stations.

¹H-NMR analysis comparing the rotaxane with the de-threaded axle have shown that the ring component is firmly bound to the ammonium station, but it starts shuttling between the two triazolium stations after the ammonium deprotonation. The reason behind this behavior is the different binding affinity of the ammonium and ammine station relative to the triazolium.

To demonstrate the ring shuttling between the two triazolium stations, ¹H-NMR spectra at different temperatures were acquired: at room temperature, two sets of signals are present for the triazolium groups and neighboring protons, indicating the shuttling is taking place is slow on the NMR timescale. At 338 K, the two signals coalesced into one as the shuttling movement became faster.¹⁴

The shuttling of the ring relative to the axle leads to a new form of conformational isomerism, where the different possible arrangements of the components relative to each other are called *co-conformers*.¹⁵

In the previously cited rotaxane made by Leigh and Lewandowski, the two co-conformers resulting from the shuttling movement are not distinguishable, thus they have the same energy. However, in case of “asymmetric” rotaxanes, with different recognition groups on either side, co-conformers with different energies are obtained. The equilibrium of the translation movement forms preferentially the more stable of the two, called ground-state co-conformer (GSCC), while the other constitutes a higher-energy metastable co-conformer (MSCC).¹⁶

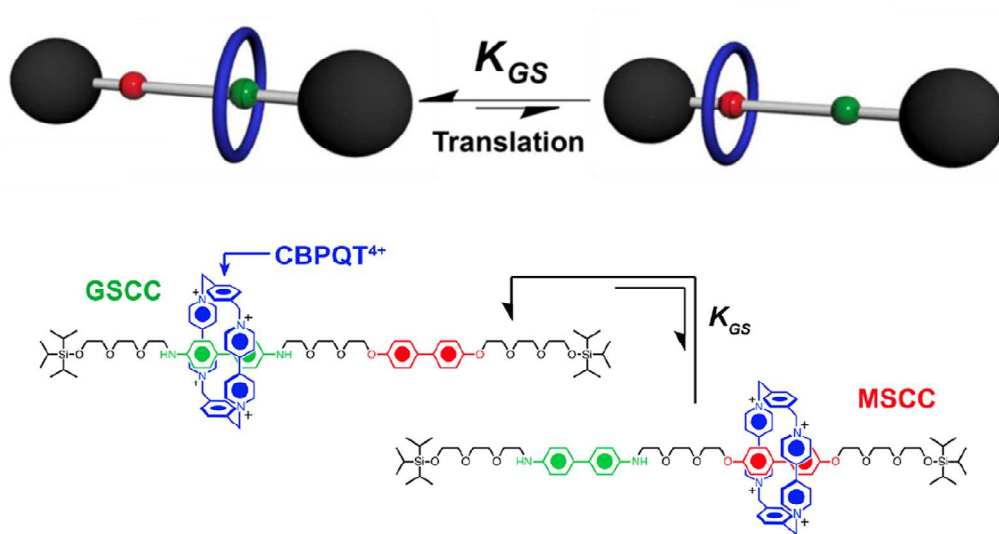


Figure 5. representation of the equilibrium between the stable ground-state, favored, co-conformer (GSCC) and the higher-energy metastable co-conformer (MSCC).

1.3 Chirality

On a rigorous approach, chirality can be assessed considering the symmetry operations (reflection, rotation exc...) that can be performed on a tridimensional object, such as a molecule. In particular, an object (molecule) is said to “possess” a symmetry operation when the product of the rearrangement after applying the operation is indistinguishable from the starting structure. On this ground, a molecule is said to be “chiral” when it lacks a mirror plane (σ), a center of inversion (i) or a rotation-reflection axis of a higher order (S_n).¹⁷ The result of the absence of these symmetry operations is that chiral molecules are not superimposable to their mirror images and, thus, exist as pairs of non-superimposable structures called “enantiomers”. Enantiomers, in fact, display the exact same connectivity between atoms (chemical formula and order of bonds), which results in maintaining identical physical and chemical properties. However, opposite enantiomers can be distinguished since they interact differently with polarized light. Specifically, they rotate the plane of polarization in opposite directions. Generally, chirality occurs when a stereogenic element is present within the molecular structure.¹⁸ The most common and easily recognizable among these is a tetrahedral carbon atom with four different substituents. This carbon atom is said to display a point chirality element and is called stereogenic center or stereocenter. If a stereocenter is present the molecule cannot display a plane of symmetry or a center of inversion and is, thus, chiral. Other stereogenic elements are axial, planar or helical (Figure 6).¹⁹

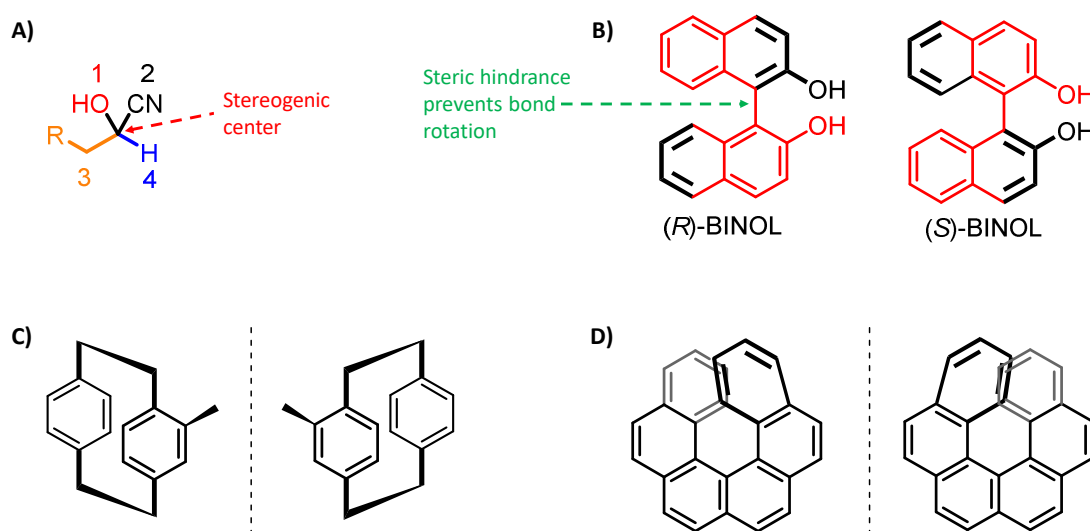


Figure 6. representation of four stereogenic elements within a chiral molecule: A) point chirality of a tetrahedral carbon atom with four different substituents; B) axial chirality due to a hindered rotation about a single bond; C) planar chirality in a cyclophane and D) helical chirality of helicenes.

When different stereogenic elements (i.e., “n” stereogenic centers) are present within the same molecule, the combinations of the possible different configurations of these centers produce up to 2^n distinct stereoisomers (Figure 7). These are called diastereomers and exist as pair of enantiomers when they lack a plane of symmetry. Interestingly, the non-mirror images diastereomers are different molecules and can display distinct physical and chemical properties. For instance, they can be separated chromatographically and display different spectroscopic features. A particular case arises when a diastereomer shows a plane of symmetry. In fact, the presence of a symmetry operation, renders the molecule achiral and the two supposed “enantiomers” are effectively the same molecule and are called “meso” forms.²⁰

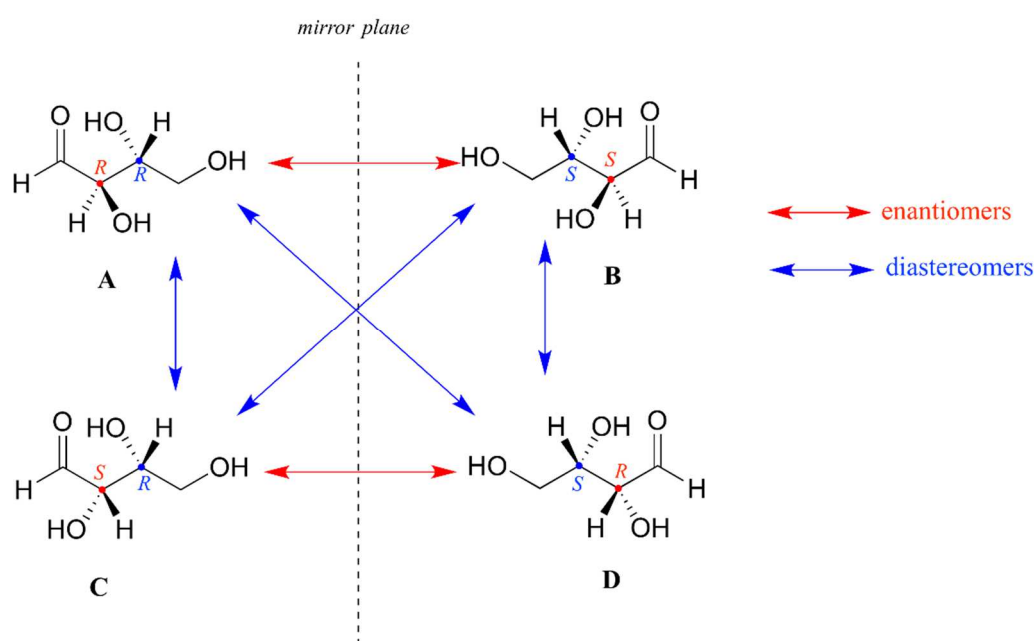


Figure 7. representation of all diastereomers arising from a molecule with two stereocenters.

In biological systems, chirality plays a crucial role. The most striking manifestation of this is the consideration that most natural chemical species are homochiral, namely, they exhibit one out of the (many) possible absolute configurations. For example, all naturally occurring amino acids are *L*-configured, while carbohydrates are *D*-configured. Interestingly, this is also reflected in further stereogenic elements, such as the helicity of α -helices formed upon proteins folding.²¹

Since one of the aims of the MIMs research effort is mimicking existing natural molecular machines, chirality must not be overlooked when designing artificial systems. Moreover, for several applications, particularly those in the pharmaceutical field, it is of paramount importance to discriminate between optical isomers since different enantiomers may exhibit,

for example, different biological activity. To this end, asymmetric synthesis methods have been developed to obtain chiral compounds preferentially in one configuration. The principle at the basis of asymmetric synthesis is that each reaction of formation of stereoisomer should proceed at a different rate. This is achieved, generally, by introducing additional chiral information in order to desymmetrize either the ground or the transition state of the reaction, transforming indistinguishable enantiomers into “distinguishable” diastereomers or diastereomeric transition states.²²

A way of measuring the purity of a chiral substance is the “enantiomeric excess”, which is defined as the absolute difference between the mole fraction of each enantiomer.²³

$$ee = |\chi_R - \chi_S| \text{ where } \chi_R + \chi_S = 1$$

although it is more often expressed as a percentage:

$$\%ee = (|\chi_R - \chi_S| \cdot 100)$$

1.4 Mechanically Planar Chirality

While the mechanical bond in MIMs allows large amplitude relative motion of the molecular components, it also creates a constriction between the interlocked components that limits the possibilities for their mutual arrangement. It is, thus, possible to create interesting outcomes displaying chirality. For example, chiral MIMs can be obtained interlocking achiral components. Specifically, let us consider an axle with a pseudo- $C_{\infty v}$ symmetry, namely having an axle of rotation coinciding with the axle, and a macrocycle whose only element of symmetry is a reflection through the plane that contains the macrocycle, that is with C_s symmetry. Such a macrocycle is also termed “oriented”. By surrounding the axle component, with the oriented macrocycle, the resulting rotaxane shows a lower symmetry and can be chiral.²⁴

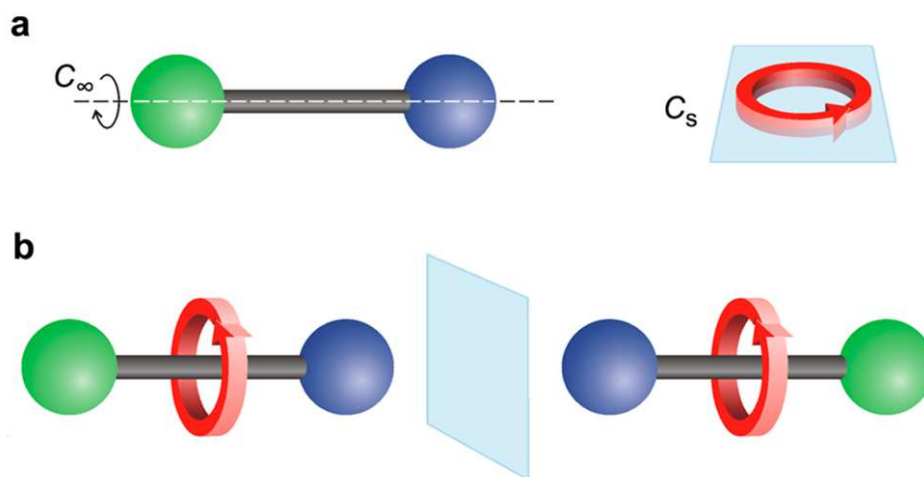


Figure 8. Schematic representation of a) an axle with C_∞ symmetry and a ring with C_s symmetry; b) the two enantiomers of a mechanically planar (MP) chiral rotaxane originated from the interlocking of the two components.

This new form of chirality displayed by rotaxanes is called mechanically planar chirality and could be exploited in several applications ranging from catalysis to sensing.²⁵

The enantioselective synthesis of mechanically planar chiral rotaxanes is highly challenging. Some recent examples from Goldup and coworkers exploited chiral adducts and provided relatively high enantioselectivities.²⁶ However, the more common approach is still to resolve enantiopure rotaxanes from a racemic mixture obtained from a non-stereoselective synthesis. One of the first example of optical resolution was developed by Jäger and Vögtle in 1997 and it was based on chromatography using a chiral stationary phase HPLC.²⁷ At the present day, there are strong limitations in obtaining enantiopure mixtures of chiral MIMs and further research is needed.

1.5 On-off switching of chirality

A particular case of MP chiral [2]rotaxanes can be obtained when the C_s symmetry ring is compartmentalized on either side of the axle with identical extremities. It is, thus, the non-central positioning of the macrocycle which desymmetrizes the structure. Positioning the oriented macrocycle on the opposite sides of the axle gives rise to two energetically equivalent mirror-images co-conformations that are, thus, enantiomeric (Figure 9). A peculiar feature of these systems is their highly dynamic character. In fact, without any “obstacles”, the ring can shuttle between the two extremities of the axle, thus, converting one enantiomer into the other

and *vice versa* by passing through an achiral intermediate situation where the ring is located at the center of the structure.²⁴

The correlation between co-conformational dynamics and chirality prompted an investigation on a way to switch the molecular shuttling through stimulation and enable MP chirality. An example has been provided by our group, where a [2]rotaxane is able to switch reversibly between a prochiral and a chiral state through chemical stimulation. This rotaxane is composed of an oriented DB24C8 crown ether macrocycle and an axle with a central dibenzilammonium station flanked by two identical methyl-triazolium stations.²⁴

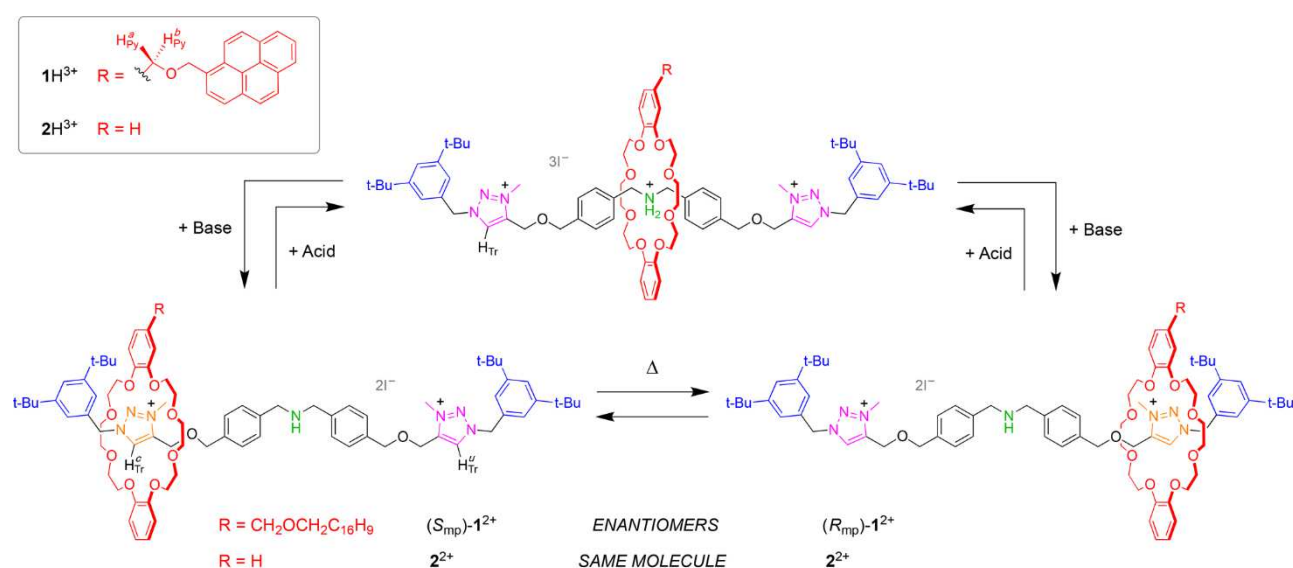


Figure 9. representation of an acid/base on-off switching of mechanically planar chirality in a rotaxane. The prochiral rotaxane (top) produces to two enantiomeric co-conformations upon deprotonation of the central ammonium station.

When the amine is protonated the ring resides preferentially on the central ammonium station due to the strong hydrogen-bond interaction. In this co-conformation the plane of reflection of the ring and of the axle coincide and the structure is achiral, or more specifically, *prochiral*. The deprotonation of the ammonium group serves as chemical stimulus to switch the ring position to the triazolium stations. Since these are identical, the prochiral structure gives rise to a 50:50 population of two energetically equivalent mirror-images co-conformers. The ring shuttling between the two identical triazolium stations interconverts the two enantiomeric co-conformations and is, thus, equivalent to a racemization reaction. Moreover, the possibility to shift the equilibrium of the racemization reaction in favour of one co-conformation. Such “bias” was obtained by having an additional stereogenic element participating in the equilibrium. In fact, the addition of an optically active anion, (1S)-(+)-10-camphorsulfonate, as a counter-ion

to the triazolium groups resulted in the formation of two diastereomeric salts in a ratio of 80:20 which reflects their energy difference. Effectively, this was the first example of *chiral resolution* of two enantiomeric co-conformations in a mechanically planar chiral rotaxane.²⁴

1.6 Kinetic Resolution

While *chiral resolution* exploits the difference in stability *at the ground state* between two diastereomeric products of a reaction with a chiral reagent, *kinetic resolution* is a method to separate enantiomers based on their difference in reactivity (*transition state*) with a chiral reagent or catalyst. Kinetic resolution is at the basis of most asymmetric synthesis methods. By definition, the two starting enantiomers have the same energy (in the case of a chiral catalyst, the same can be said for the two products). The key aspect lies in the difference in the stability of the two diastereomeric transition states (TS). The reaction proceeds faster via the pathway with the lower activation energy, or the more stable TS. Therefore, one of the two enantiomers reacts faster than the other, as a result the mixture of products shows a certain degree of selectivity toward that enantiomer, namely a non-zero enantiomeric excess. The selectivity of a kinetic resolution can be quantitatively expressed in terms of the kinetic constants for the “R” and “S” reactions (k_R and k_S).

$$s = \frac{k_R}{k_S} = e^{\Delta\Delta G^\ddagger/RT}$$

From the equation above it is clear that selectivity is high when k_R are markedly different k_S , or in other words when the difference in Gibb's free energy of activation between the two transition states ($\Delta\Delta G^\ddagger$) is high.

In general, there are two types of kinetic resolution methodologies, classical (KR) and dynamic kinetic resolution (DKR).²⁸ Their difference lays in the height of the energy barrier for the conversion between the two enantiomers with respect to the activation barrier of the resolution reaction (Figure 10).

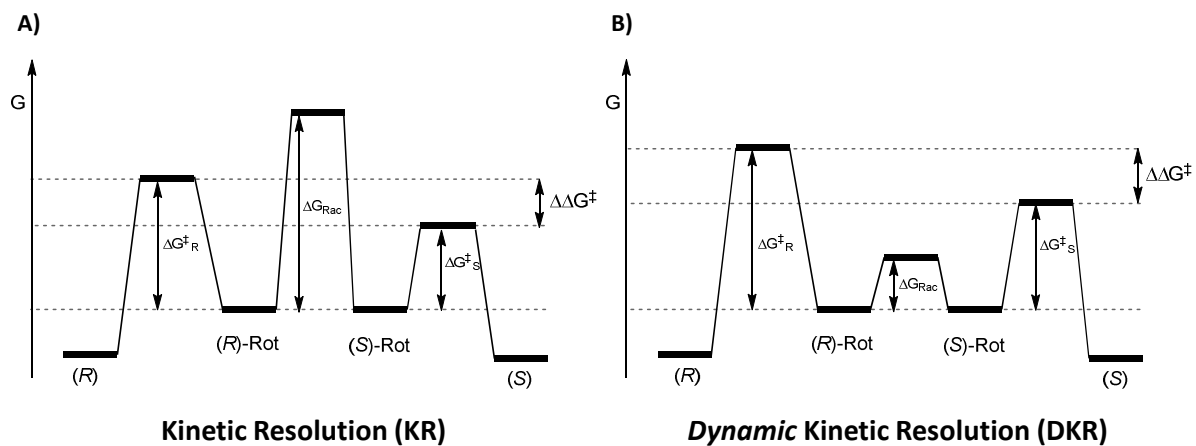


Figure 10. energy diagrams representing A) a classical kinetic resolution (KR) and B) a dynamic kinetic resolution. It can be noticed how KR and DKR differ in the activation energy of the process of racemization of the two enantiomers (ΔG_{Rac}).

Classical kinetic resolution

When the energy barrier for the interconversion of the two enantiomers is higher than those of the resolution reactions, we speak about classical *kinetic resolution* (Figure 10A). The main limitation is that interconversion between enantiomers is prevented. This, in combination with a high selectivity (large $\Delta\Delta G^\ddagger$), allows only one enantiomer to undergo the resolution reaction. Therefore, a maximum yield of 50% of the desired optically pure product can be obtained when starting from a racemic mixture.²⁸

A successful example of application of the KR strategy to the resolution of MP chiral rotaxanes was reported recently by Kawabata *et al.* They developed an enantioselective acylation of a MP chiral rotaxane. Since the two enantiomers cannot be interconverted, therefore the procedure is a classical KR.

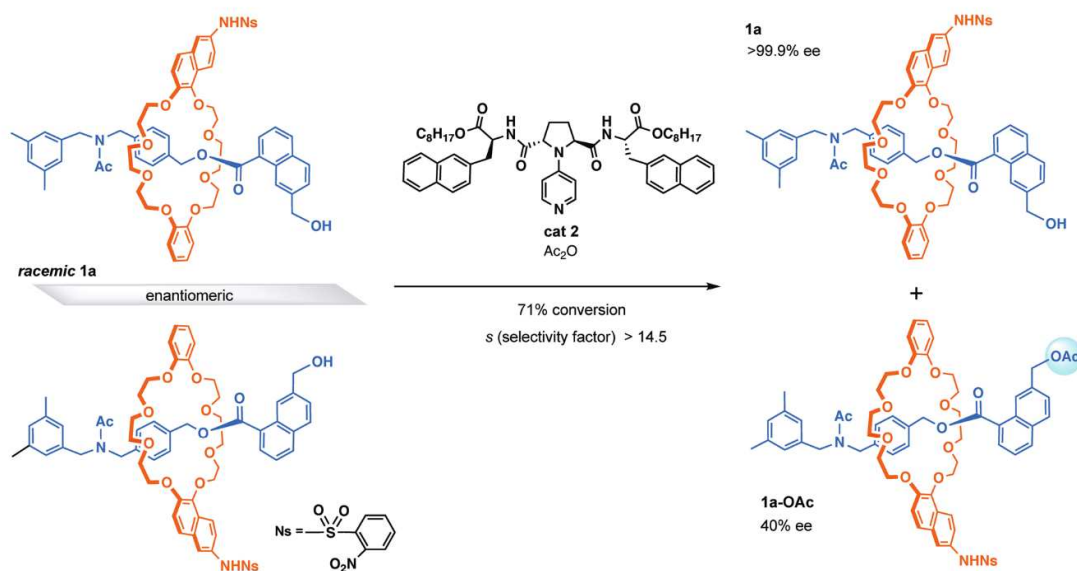


Figure 11. kinetic resolution by Kawabata *et al.*²⁹ over a racemic mixture of mechanically planar enantiomers of a rotaxane, performed by an organocatalyzed asymmetric acylation.

In this work, an enantiomeric excess of 99.9% was obtained using a chiral catalyst which took part in the acylation of a terminal hydroxyl group located on the axle. The high efficiency of the remote catalysis was unexpected, considering the distance between the active site (pyridine nitrogen) from the chiral components. A possible explanation to this behavior can be motivated by considering an interaction between the catalyst chiral groups and the substituent of the oriented macrocycle.²⁹

However, the high ee was obtained with the low yield of 29%, which recalls the limitations of the classical kinetic resolution, namely the theoretical maximum yield of 50%.

Dynamic Kinetic Resolution

When two enantiomers can interconvert between each other at a faster rate than the asymmetric reaction, we speak about *Dynamic Kinetic Resolution* (Figure 10, B). Also in this case, the enantiomer with the lower activation barrier reacts faster, but the interconversion reaction is fast enough to replace the reacted enantiomer with the unreacted one. It is clear, considering the Le Chatelier principle for the racemization equilibrium, that the “wrong” enantiomer is also driven to the “correct” product regardless of the initial thermodynamic distribution dictated by the equilibrium constant. In fact, for DKR, the Curtin-Hammet principle holds true.³⁰ This principle tells us that the products distribution, when two reaction pathways are available (i.e., asymmetric reactions), is dictated solely by the difference in the Gibbs’ energy of the transition states for these two reactions. For these reasons, thanks to the combination of asymmetric and interconversion reactions DKR can reach a theoretical yield up to 100%.

It is noteworthy that, to date, no DKR strategy has been reported for the resolution of mechanically planar chiral rotaxanes.

2. AIM OF THE THESIS

The first objective of this research project is to prepare and investigate the molecular switching behaviour of two mechanically planar (MP) chiral rotaxanes. These rotaxanes are composed of a symmetric axle and an oriented (C_s symmetrical) dibenzo-24-crown-8 ether bearing different flanking functional groups. The axle comprises a switchable ammonium station which can be deactivated upon treatment with a base enabling ring shuttling to the two equivalent triazolium secondary stations toggling the MP chirality.

The second objective of this thesis is to investigate strategies for obtaining diastereomeric structures including one MP stereogenic element and (at least) one stereocenter. The functionalization of the axle with a chiral group in a position that inhibits the ring shuttling between the two triazolium stations (stoppering) should afford two configurationally stable mechanically planar chiral [2]rotaxanes. The development of accurate methods of analysis is also an integral part of this objective. Briefly, starting from the mechanically planar chiral [2]rotaxane with the oriented DB24C8-type ring, we plan the addition of an optically pure chiral group to the central amine recognition station to halt the shuttling – and the interconversion between enantiomers – and also introducing an additional a stereocentre to the already present MP chirality. This results in the formation of two distinct diastereomers that could, potentially, be observed as distinct species by NMR. Two reactions will be investigated and optimized toward this end, namely amide and sulfonamide bond formation. Moreover, NMR conditions to distinguish the diastereomers will be optimized through variation of solvents and temperatures.

Finally, we foresee the possibility that the two configurations of the MP chiral [2]rotaxanes could react at different rates with the optically pure (sulfon)amide precursor, resulting in a product exhibiting a non-zero diastereomeric excess and effectively realizing a kinetic resolution of the MP enantiomers.

3. RESULTS AND DISCUSSION

3.1 Synthesis and purification of the asymmetric [2]rotaxanes

The mechanically planar chiral rotaxanes **1aH⁺** and **1bH⁺** were prepared via the following multistep route: first the rings (**A** and **B**) and axle precursor (**4**) were synthesized, and secondly the rotaxane were prepared via a *stopping* reaction exploiting a passive templated strategy taking advantage of the ammonium-crown ether supramolecular threaded complex. The final step consists in the activation of the triazole moieties converting them in triazolium recognition stations through methylation reaction. Purification of each intermediate was performed prior taking it to the subsequent step.

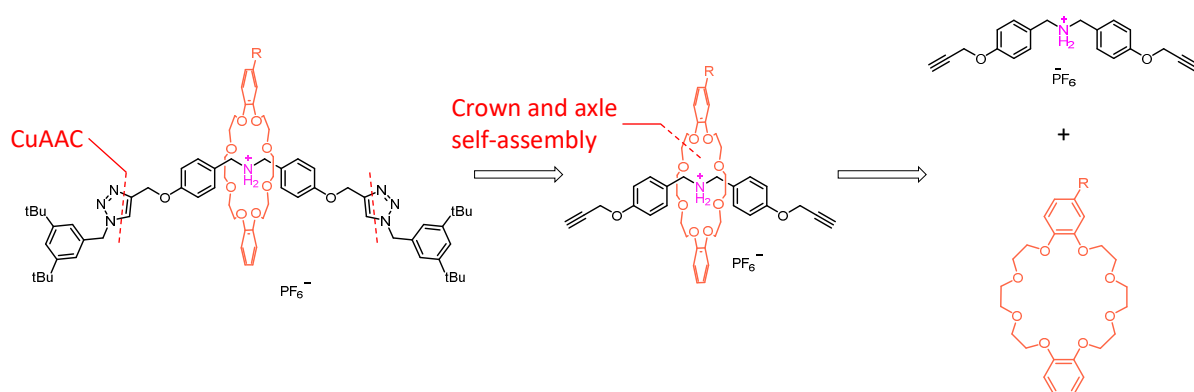


Figure 12. retrosynthesis of the target [2]rotaxane. The pseudo-rotaxane structure, obtained via self-assembly, undergoes a regioselective 1,3-dipolar cycloaddition at the extremities, adding two bulky stoppers that prevent the dethreading of the macrocycle.

3.2 Synthesis of the axle precursor

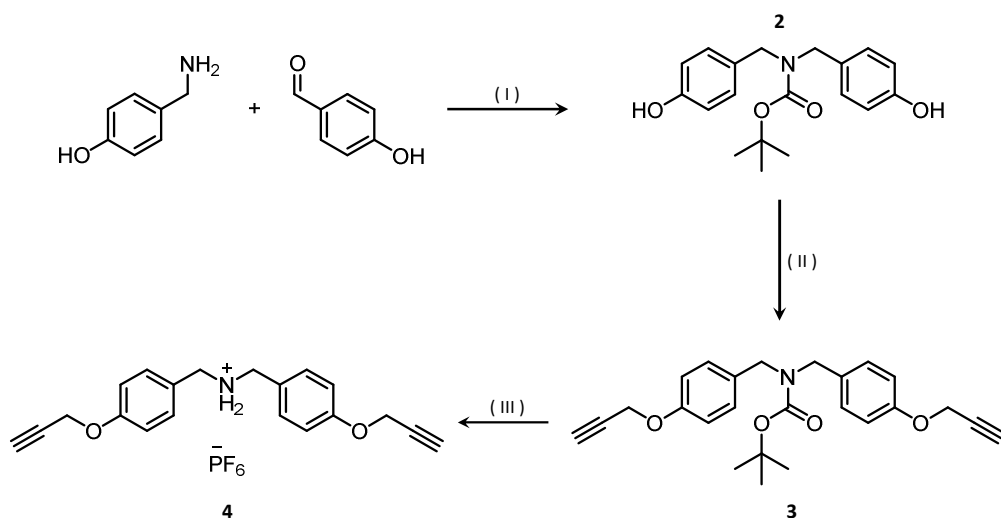


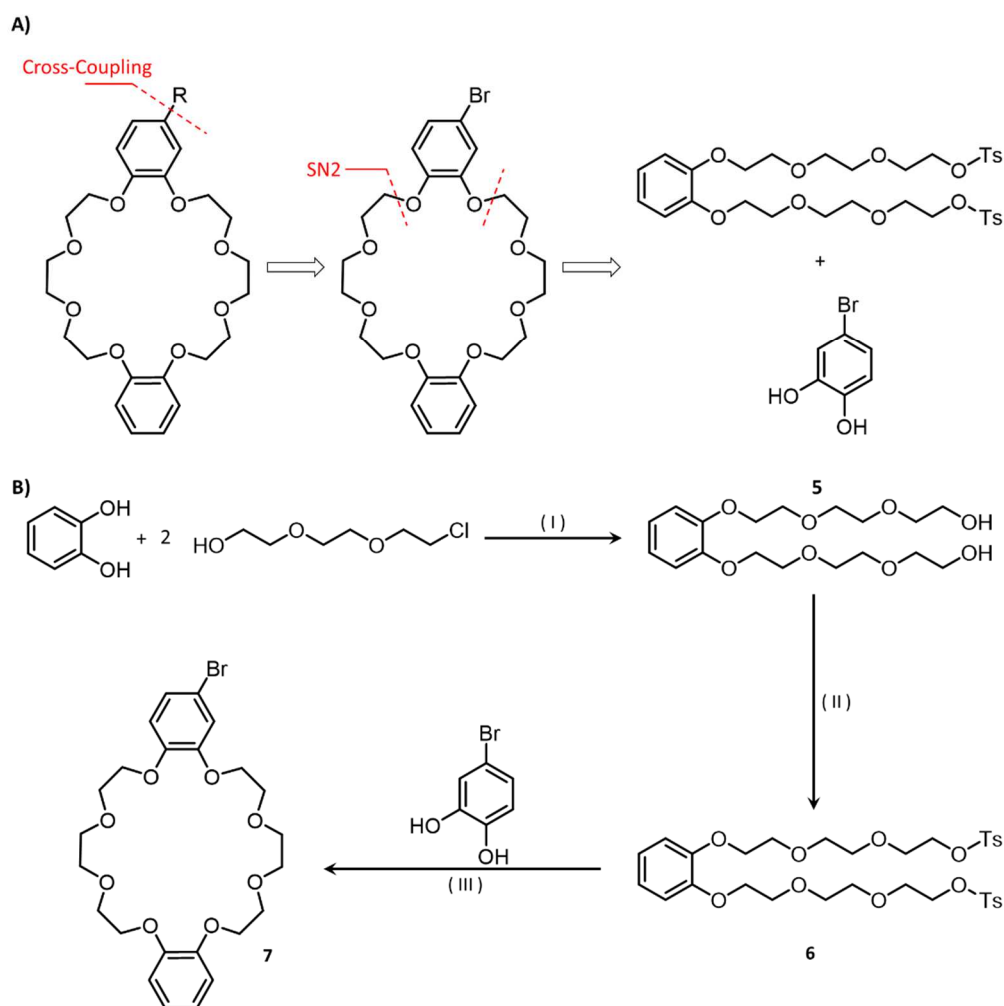
Figure 13. scheme of the synthetic route to compound **4**. **I**) a) EtOH, rotavapor b) NaBH₄, MeOH. 81% c) Boc₂O, THF r.t. quant. **II**) Propargyl bromide, K₂CO₃ CH₃CN (dry). 94% **III**) a) TFA, DCM., 25 °C b) NaHCO₃, 75% c) MeOH, HCl d) NH₄PF₆ (sat), acetone.

The central portion of the axle (**4**), which contains the ammonium recognition station was prepared starting from commercially available starting materials. All the steps were optimised to provide a relatively high yield, allowing the production of large quantities of the axle precursor that can be subsequently stored and readily used to prepare the [2]rotaxanes upon complexation and stoppering.

The first step is the reductive amination of 4-hydroxybenzaldehyde and 4-hydroxybenzylamine to yield 4,4'-hydroxydibenzylamine, which is subsequently protected with a *t*-Butyloxycarbonyl (Boc). The protection of the amine moiety is necessary to ensure regioselective propargylation of the hydroxy groups. Deprotection in acidic conditions and subsequent anion exchange yielded the desired ammonium product as hexafluorophosphate salt. The product in its salt form is bench stable and can be stored and used readily for the subsequent synthetic steps.

3.3 Synthesis of the “oriented” crown ethers

The synthesis of the functionalised crown ethers is a slightly more challenging compared to the axle. Our strategy involves the late-stage functionalization of a common DB24C8 precursor. In this way we can ensure that a wide variety of substituent groups could be attached to the main structure of DB24C8. In order to achieve this, our main course of action was to produce a crown ether precursor bearing a handle for further functionalization. In this case, a bromide moiety was selected, as it allows a wide range of reactions, in particular sp^2 - sp^2 cross-couplings.



Two different C_s symmetric macrocycles were synthesized bearing a 3,5-bis(trifluoromethyl) benzene (**A**) or a dimethyl-*t*-butylsilyl alkyne (**B**) functional groups. We envisioned that these groups could be beneficial in the monitoring the diastereoisomers formation by NMR

spectroscopy. Specifically, the trifluoromethyl groups in ring A resonate as a sharp singlet in the ^{19}F NMR spectrum, while the methyl groups of the silane functionality in ring B resonate at very high fields in the ^1H NMR spectrum. Moreover, upon deprotonation of the rotaxane and installation of the co-conformational mechanically planar chirality, these two methyl groups become diastereotopic, thus should be distinct in the NMR spectrum.

The synthesis has been previously optimized in the group to provide high yields and multigram quantities of the desired macrocyclic precursor (**7**). The synthesis starts with the functionalization of catechol with triethyleneglycol chains, which proceeds via nucleophilic substitution. The free hydroxy groups of the intermediate are then converted into 4-toluenesulfonate esters in order to undergo a second nucleophilic substitution during the macrocyclization step. In this case, the macrocyclization reaction was carried out with a catechol-based reagent, 4-bromocatechol, to obtain the common ring precursor **7**.

In order to favour macrocyclization over oligomerization, the nucleophilic substitution reaction is carried out under high dilution ($C < 0.1\text{ M}$), by slow addition of a solution of open intermediate and 4-bromocatechol in a refluxing suspension of Cs_2CO_3 in THF. Moreover, the Cs^+ ions template the formation of the macrocycle coordinating the oxygen atoms of the triethylene glycol chains.³¹

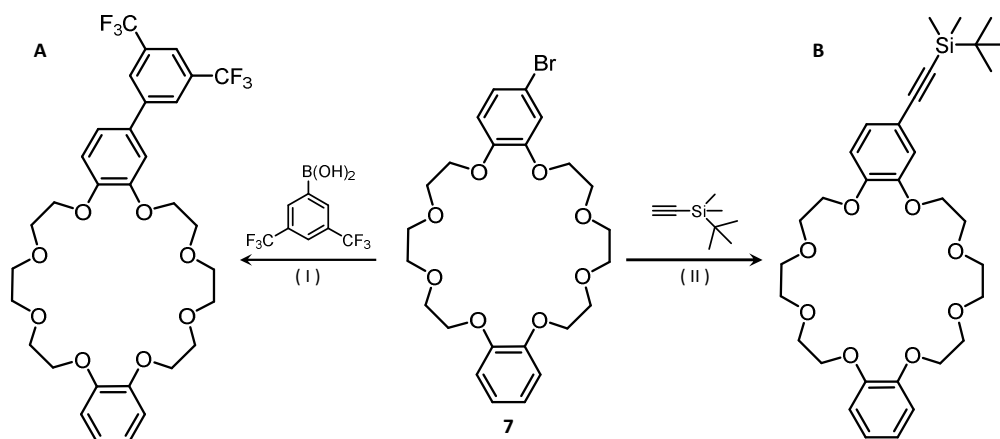


Figure 15. Synthetic route to the compounds **A** and **B**. I) $\text{Pd}(\text{PPh}_3)_4$, K_2CO_3 – “Suzuki”; II) $\text{Pd}(\text{PPh}_3)_4$, CuI , DMF , *Diisopropylamine*, 85°C , N_2 reflux – “Sonogashira”.

As previously specified, compound **7** is a versatile precursor to a wide variety of oriented macrocycles. Specifically, compound **A** was synthesized by Suzuki cross-coupling with 3,5-trifluoromethylphenylboronic acid. The reaction is catalyzed by $\text{Pd}(0)$ and proceeds according to the catalytic cycle depicted in figure 16, A.

On the other hand, compound **B** was prepared by Sonogashira cross-coupling with dimethyl-*t*-butylsilyl acetylene. The Sonogashira cross-coupling allows to selectively form a carbon-carbon bond between an arene and a terminal alkyne group. The reaction is Pd(0) mediated and require the presence of Cu(I). The key intermediate is the organocuprate formed in situ upon coordination of Cu(I) with the alkyne. The complete catalytic cycle is depicted in figure 16B. It is noteworthy that the reaction has to be ran under strictly oxygen free atmosphere in order to avoid oxidation of the catalytic competent Cu(I) to the inactive Cu(II). Specifically, oxygen was removed by freeze-pump-thaw cycles and the reaction was then kept under a nitrogen atmosphere.

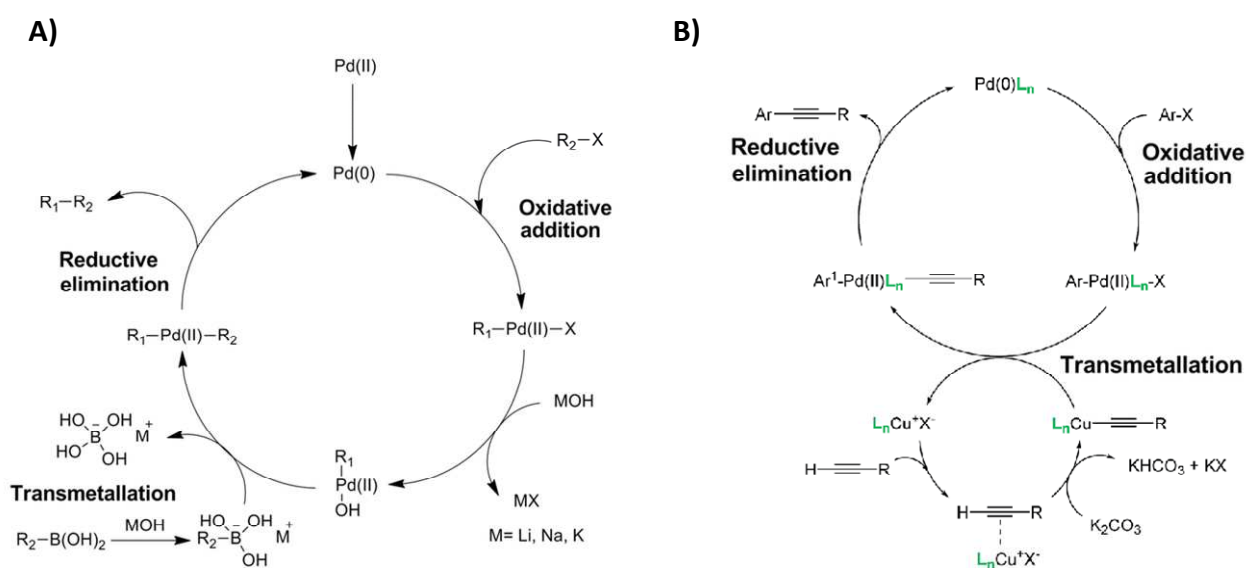


Figure 16. Schemes of the catalytic cycles for Suzuki (A) and Sonogashira (B) cross-coupling reactions.

3.4 Synthesis of prochiral rotaxanes 1a and 1b

The synthesis of the rotaxane interlocked structure was performed via a passive templated strategy which involves a *stopping* reaction on a preformed threaded complex which “traps” the macrocycle in the dumbbell-shaped axle. As mentioned in the first chapter, *stopping* is the most common synthetic route developed for the preparation of rotaxanes.

The key step is, thus, the formation of the pseudo-rotaxane complex precursor which occurs by *self-assembly* of compound **4** and the chosen macrocycle (either DB24C8, **A** or **B**) in a suitable solvent. In this case, the driving force for the *self-assembly* step is the formation of a network of hydrogen bonds between the oxygen atoms of the macrocycle and the ammonium station of

compound **1a**. Therefore, it can be associated to the complexation equilibrium reported in figure 17.

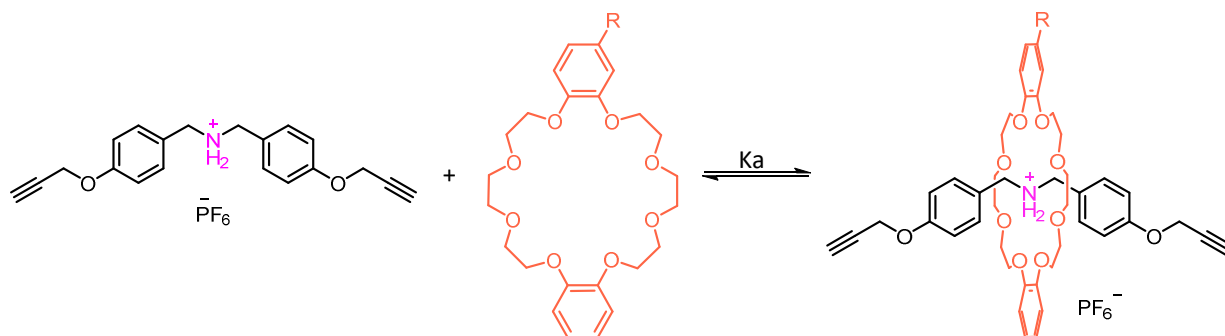


Figure 17. representation of the self-assembly mechanism as the complexation equilibrium of the central ammonium station located on the axle precursor.

Choosing the right solvent is crucial to shift the equilibrium toward the complex. In particular, the solvent needs to ensure good solubility of the (charged) reagents, while at the same time avoid competition with the hydrogen bond formation. For this purpose, the solvent should be aprotic and have a relatively low polarity. Additionally, the use of the non-coordinating hexafluorophosphate anion as the counterion of the positively charged ammonium improves the solubility of the salt in organic media. For instance, aromatic solvents such as benzene greatly favour the hydrogen bond formation but at the expense of solubility of the compounds. A good compromise is dichloromethane, which combines good solubility with a very high complexation constant ($K_a > 10^6 \text{ M}^{-1}$). Moreover, to ensure full complexation under reaction conditions, the equilibrium is pushed even further toward products adding two equivalents of macrocycle. The reason behind the necessity of maximising the complex formation is that the subsequent stoppering reaction generally takes place preferentially with the free compound **4** for steric reasons.

The following step, which is a formal 1,3-dipolar cycloaddition catalysed by Cu(I) (copper-catalysed azide-alkyne cycloaddition or CuAAC) between the terminal alkynes of the complex and 3,5-di-*t*-butyl benzylazide that adds the bulky stoppers to the axle and forms the interlocked structure. The reaction is catalyzed by Cu(I) – $[\text{Cu}(\text{CH}_3\text{CN})_4]\text{PF}_6$ – which proceeds under mild conditions and have excellent regioselectivity toward of the desired 1,4-substituted 1,2,3-triazole moiety. Although heating is generally beneficial for this type of 1,3 dipolar cycloadditions, it was avoided as it would decrease the association constant due to an increase in the entropic contribution to the ΔG . In fact, the complexation reaction has a negative free energy (ΔG) which mostly comes from a negative enthalpy value (ΔH) due to the formation of hydrogen bonds. However, the entropic term (ΔS) is positive as we are decreasing the number

of species. Upon increasing the temperature, the $T\Delta S$ increases rendering the ΔG less negative (as $\Delta G = \Delta H - T\Delta S$) thus pushing the equilibrium towards reagents.

Similarly to the Sonogashira cross-coupling, also the CuAAC needs to be performed under air-free atmosphere in order to prevent oxidation of the Cu(I) catalyst. For this reason, the reaction mixture was degassed by purging it with nitrogen for at least 20 minutes and the reaction was then kept under a nitrogen atmosphere. Interestingly The catalyst integrity can be visually checked from the colour of the solution: a green colour, is indicative of the presence of the catalytically competent Cu(I) complex. On the other hand, a blue colour is indicative the formation of Cu(II) inactive species. Since the optimized conditions required the reaction mixture to be stirred for a week, an unusually large amount of it is added to the reaction mixture (0.8 equivalents), to make up for the exhausted catalyst.

Together with rotaxane **8**, the crude product contains surely free macrocycle and unreacted azide, as they were used in excess, along with all the by-products such as the free axle. The separation of these species was attempted with a silica gel column chromatography, but the preliminary TLC analysis shows a strong overlap between all the components together with an elongated shape of the spots. A more effective method of carrying out the separation turned out to be the size-exclusion chromatography (or gel-permeation chromatography, GPC) which separate the products by according to their hydrodynamic diameter. Operationally, it consists of a chromatographic column filled with a styrene-divinylbenzene resin stationary phase which forces smaller molecules to undergo a longer pathway as they get “trapped” in the porose structure, while the bigger ones take a more direct route thus eluting first and separating them from the smaller ones. Since the difference in size between the rotaxane and the impurities is relevant, GPC is highly effective to purify these molecules.

The synthesized rotaxane contains a single ammonium recognition station in the centre, to which the macrocycle is strongly bound, in light of the strong binding between DB24C8-type macrocycles and ammonium moieties. To obtain the final rotaxanes **1aH⁺** and **1bH⁺**, treatment of rotaxane **8** with methyl iodide or methyl triflate was performed selectively methylate the triazole units generating two positively charged triazolium stations (figure 18). This is highlighted in the ¹H NMR spectrum which displays a marked downfield shift of the resonance associated with the triazole protons that shift from 7.67 ppm to 8.39 ppm, together with the appearance of a singlet at 4.31 ppm associated with the -CH₃ group.

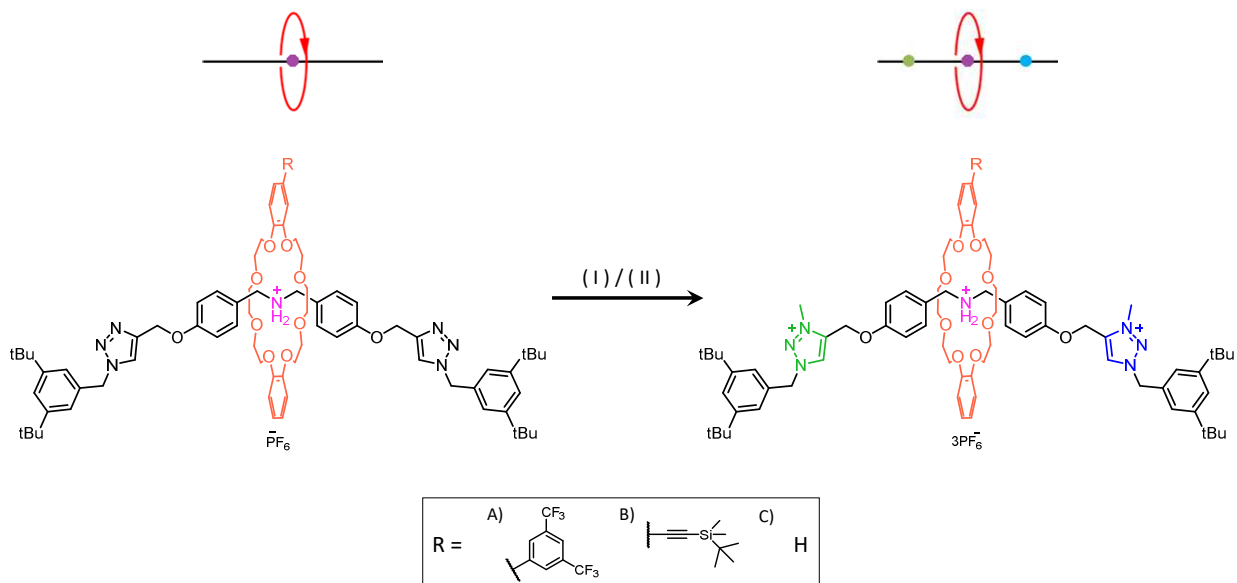


Figure 18. scheme of the methylation reaction: I) excess CH_3I , 72h; II) methyl triflate (2.5 eq), anhydrous CH_2Cl_2 , N_2 atmosphere, 0°C , 1h.

3.5 Acid/base-induced ring shuttling

The rotaxanes synthesized within this thesis are endowed with a primary ammonium station and two triazolium stations that exhibit a lower binding constant compared to the central ammonium station. These systems can, thus, undergo controlled ring shuttling between the ammonium and the triazolium stations following acid/base treatment. Because of the large difference in affinity over 99% of the rings encircle the central ammonium station. The structure has a plane of symmetry which includes the macrocycle and bisect the axle in two identical halves. In this co-conformation the rotaxanes are, thus, achiral regardless of the fact that the macrocycle is oriented. Upon treatment with a base, however, the ammonium functional group is converted to an amine, a weaker station for the ring. Macrocycles, thus, shuttle to the more favourable positively charged triazolium station. It is noteworthy that the deprotonation of the central ammonium station gives rise to two co-conformations in equilibrium *via* thermally activated ring-shuttling between the two equivalent triazolium stations (figure 19).

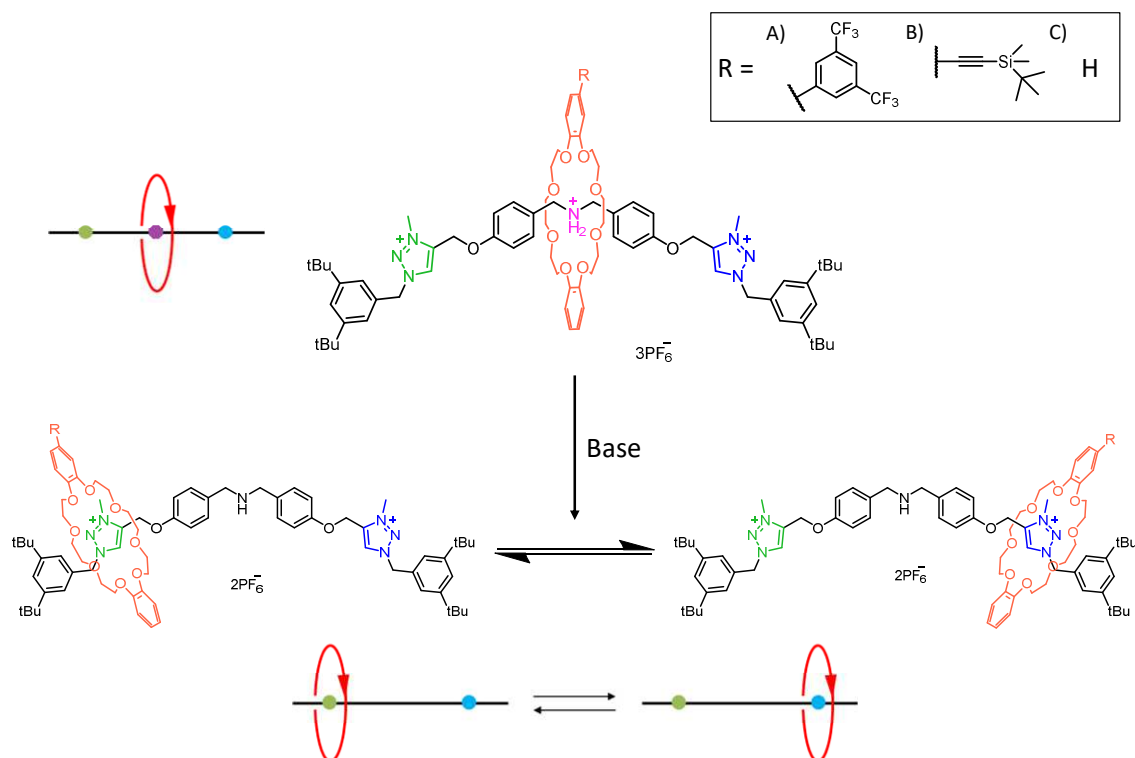


Figure 19. detailed and schematic representation of base-enabled switching of a mechanically planar chiral [2]rotaxane. The deprotonated rotaxane is shown with the two rapidly-interconverting enantiomeric co-conformers.

The deprotonation was initially performed on the symmetric [2]rotaxane **1cH⁺**. In a typical experiment, resin-bound diazabicycloundecene (DBU) was added to a solution of **1cH⁺** in CD₂Cl₂. The deprotonation was monitored by ¹H NMR following the disappearance of the signal at 4.60 ppm characteristic of the benzylic protons involved in hydrogen bonding with the macrocycle.

The presence of two equivalent co-conformations with the ring shuttling between the triazolium stations is confirmed by the presence of two resonances at 9.50 and 8.50 ppm corresponding to the encircled and unencircled triazolium respectively. Moreover, a general broadening of the peaks is observed which is indicative of an intermediate rate of exchange between the two co-conformations is in the NMR timescale. Similar results were obtained upon deprotonation of the asymmetric rotaxanes **1aH⁺** and **1bH⁺** to yield **1a** and **1b** (Figure 20 and 21).

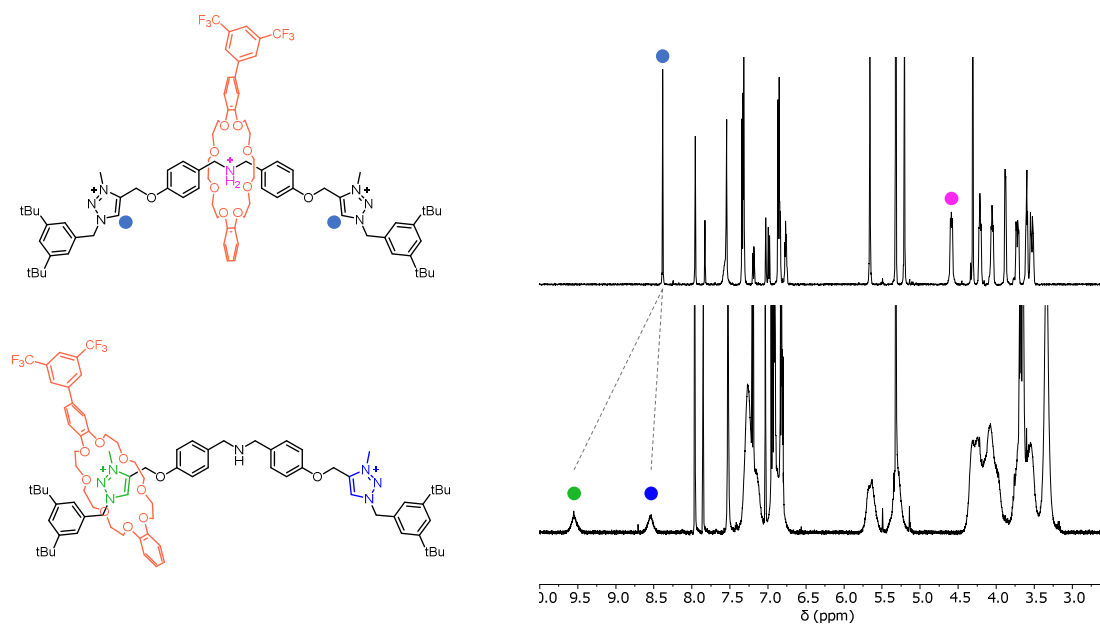


Figure 20. experimental evidence of the deprotonation of the rotaxane $1aH^+$ forming $1a$. The 1H NMR spectra show the disappearance of the signal associated with the benzylic protons nearby the complexed ammonium station (marked in magenta) and the appearance of the two broad signals of the complexed (green) and free (blue) triazolium units.

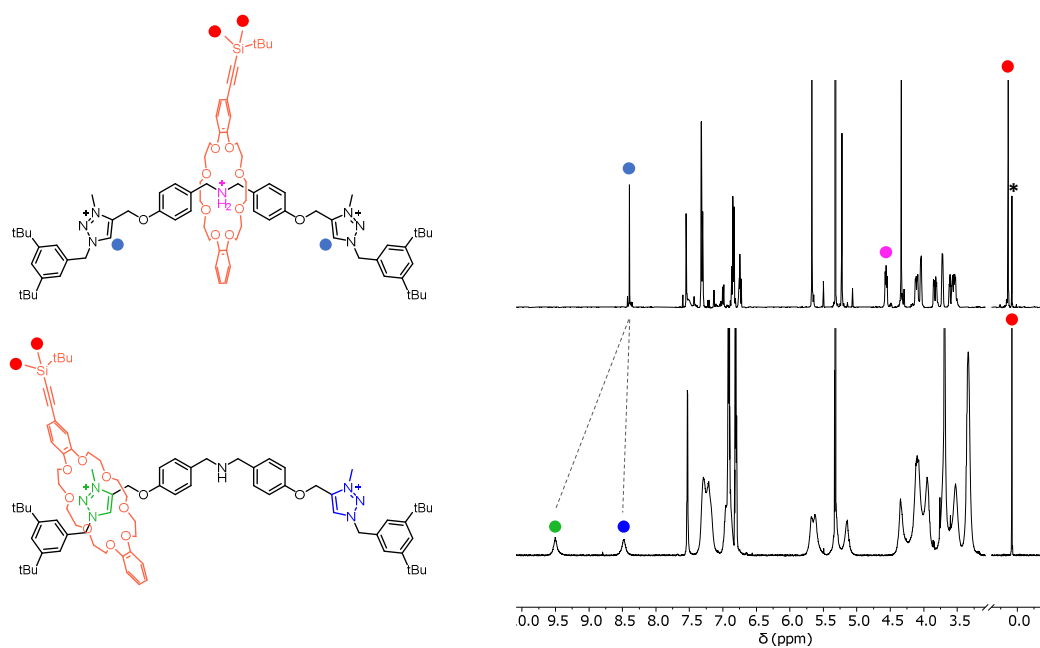


Figure 21. experimental evidence of the deprotonation of the rotaxane $2aH^+$ forming $2a$. The 1H NMR show the disappearance of the signal associated with the benzylic protons nearby the complexed ammonium station (marked in magenta) and the appearance of the two broad signals of the complexed (green) and free (blue) triazolium units. The signals associated with the diastereomeric methyl groups connected to the Silicon atom resonate at the same frequency. The signal highlighted with a "*" is an impurity.

In the case of the rotaxane **1b**, the expected splitting of the diastereotopic signals of the two silane methyl groups was not detected in the ^1H NMR spectrum after the deprotonation. Therefore, it was decided to attempt a kinetic resolution only with the rotaxane **1a**.

3.6 Kinetic resolution

In the case of the asymmetric rotaxanes **1a** and **1b**, the deprotonation of the ammonium unit, on top of toggling the shuttling movement generates two co-conformations that are energetically equivalent but mirror images, therefore they exhibit mechanically planar chirality.^{24,25} Moreover, the thermally-activated ring shuttling between the two triazolium stations converts one co-conformation into its enantiomeric.²⁴ Given the low energy barrier and the lack of stereoselectivity in the deprotonation, rotaxanes **1a** and **1b** exist in solution as a racemic mixture of the two mechanically planar chiral co-conformations.²⁴

It is noteworthy that the deactivation of the ammonium station has yet another consequence, namely to enable the reactivity at the reactive amino group, paving the way for further functionalization of the axle by nucleophilic addition. Of particular interest in the context of this thesis, is the addition of a bulky optically pure chiral stopper to the central amino group in order to block ring shuttling (figure 22), inhibiting racemization, and producing two configurationally stable diastereomers bearing a point and a mechanical stereogenic elements. To this end, functionalization of the amino group that introduces chiral groups bulky enough to act as stopper, trapping the ring on one side of the rotaxane. On top of that, a kinetic resolution approach could be envisioned that favours the reactivity of one mechanically planar enantiomer over the other, thus generating preferentially one diastereomer over the other. In this context, the structure and the dimensions of the stopper exerted great influence over the properties of the resulting diastereomers and the efficiency of the kinetic resolution.

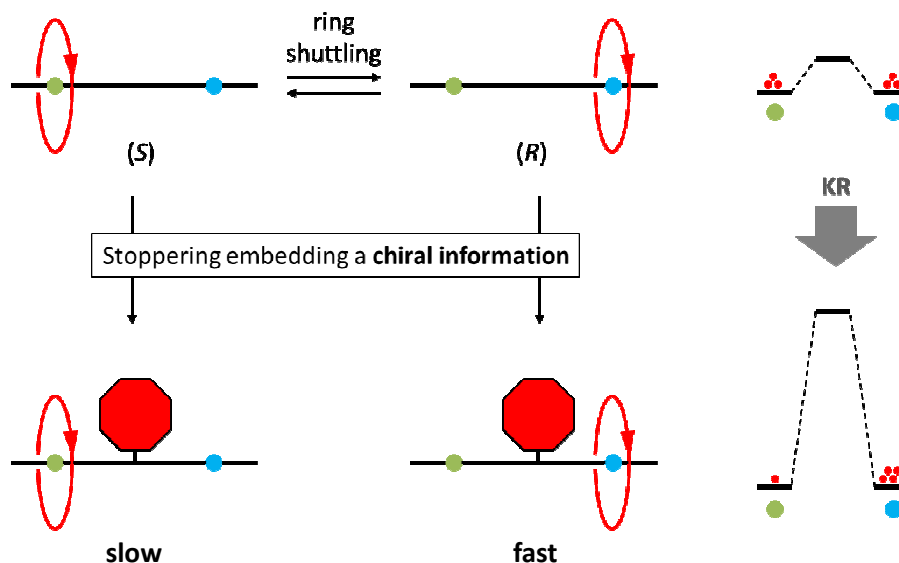


Figure 22. schematic representation of a dynamic kinetic resolution of MP chiral rotaxanes.

The functionalization of the amino group should be relatively straightforward and proceeds under relatively mild conditions. Therefore, the synthesis of amides or sulphonamides from acyl or sulphonyl chlorides, respectively, were taken as benchmark reactions. Specifically, the reactions with camphanyl chloride and camphorsulfonyl chloride were evaluated for the kinetic resolution of the mechanically planar chiral rotaxanes **1a** and **1b**.

3.7 Reaction with camphorsulfonyl chloride

The (1*S*)-(+)-10-camphorsulfonamide group represented, potentially, a good candidate for two reasons: it is large enough to act as an optically pure stopper embedding the chiral information effectively and, at the same time, it does not give rise to rotamers in the ^1H NMR spectrum due to the fast rotation of S-N bonds on the NMR timescale.³² The reaction of formation of the sulfonamide sees the rotaxane amino group acting as a nucleophile and the (1*S*)-(+)-10-camphorsulfonyl chloride as the electrophile (figure 23). A base was also added to neutralize the HCl produced by the reaction.

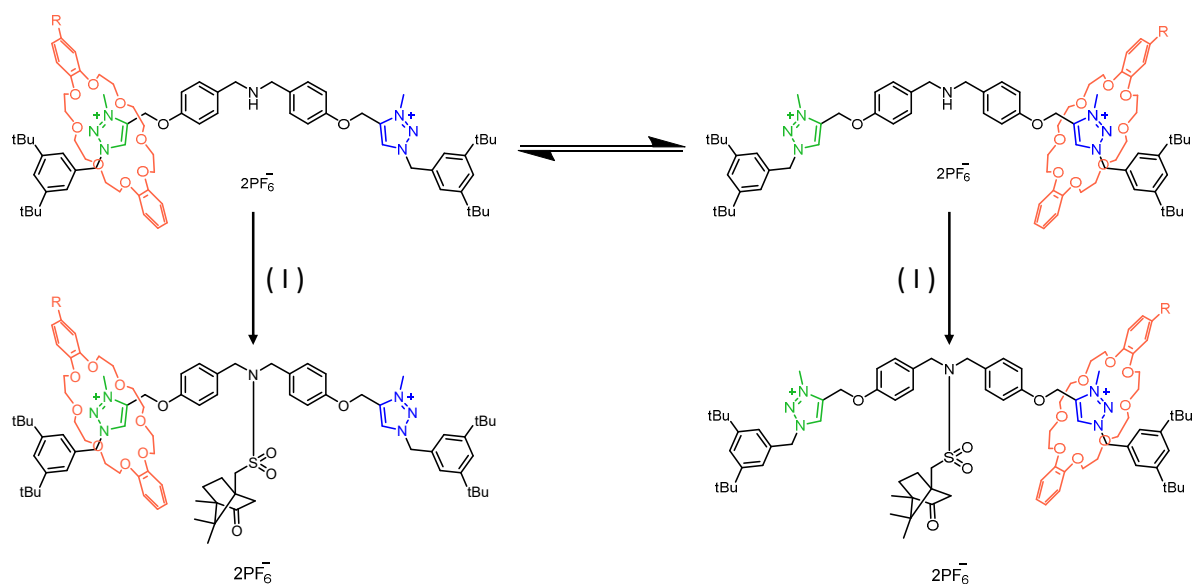


Figure 23. scheme of the reaction between the rotaxanes **1a** and **1c** and (1S)-(+)-10-camphorsulfonyl chloride: 1) (1S)-(+)-10-camphorsulfonyl chloride, base.

Given the high reactivity of the sulfonyl chloride, a stability test was performed by placing 5 mg of (1S)-(+)-10-camphorsulfonyl chloride in the presence of a strong base in the form of DBU resin to simulate the reaction conditions (where the base is needed to neutralize the forming HCl). NMR spectra were acquired before and after the addition of the base. The results revealed that the sulfonyl chloride was already partially hydrolysed prior the addition of the base, indicating strong reactivity with water. Coherently with this hypothesis, the NMR spectrum acquired after the experiment showed complete hydrolysis of the sulfonyl chloride, warning about a potential competition between hydrolysis and sulfonamide formation.

Therefore, precautions were taken to avoid the presence of water in the reaction environment, such as oven-dried glassware and anhydrous reagents and solvents.

To study the sulfonamide stoppering on the rotaxane, three test reactions were set up using deprotonated symmetric rotaxane as a model compound and (1S)-(+)-10-camphorsulfonyl chloride as the electrophile. The base effect was screened, specifically reactions were performed in the absence of base, using K₂CO₃, or DBU (figure 24, respectively A, B and C). All reactions were carried out directly in 400 µl of anhydrous deuterated dichloromethane, so the reaction mixture can be analysed immediately via NMR. The reaction mixtures were left stirring overnight and subsequently analysed through NMR spectra.

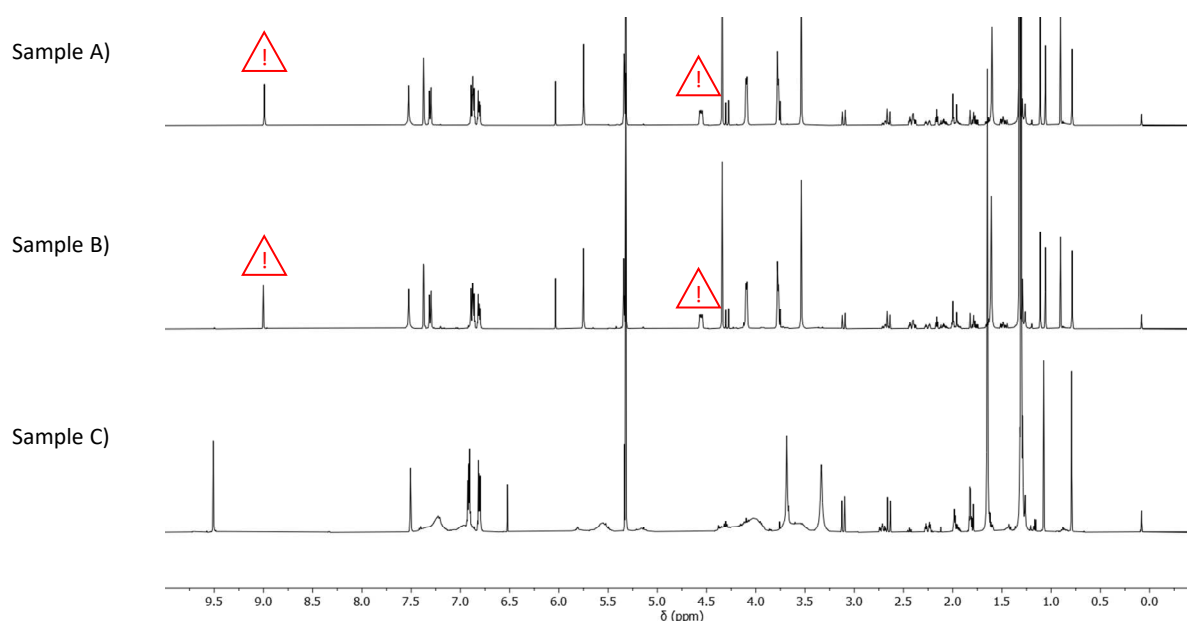


Figure 24. ^1H NMR spectra of the three reactivity experiments carried out with rotaxane **1a** and (1*S*)-(+)-10-camphorsulfonyl chloride in CH_2Cl_2 using different bases (500 MHz, 298 K): A) no base; B) K_2CO_3 ; C) DBU. Highlighted with a “!” symbol are the signals of the protonated rotaxane formed upon hydrolysis of the sulfonyl chloride.

The spectra of samples without base and using K_2CO_3 as the base, show the presence of the characteristic signal of dibenzyl ammonium encircled by the macrocycle at 4.5 ppm. At the same time only one signal is visible around 9.0 ppm, corresponding to the proton of the two equivalent unencircled triazolium stations. Additionally, signals pattern consistent with the hydrolysis of the sulfonyl chloride to sulfonic acid are present. These results indicate that the rotaxane reverted back to its protonated, achiral, form, without reacting with the (1*S*)-(+)-10-camphorsulfonyl chloride. On the other hand, when DBU was used as the base, the rotaxane underwent extensive decomposition as several characteristic signals disappeared from the ^1H NMR spectrum. This outcome is not uncommon when the rotaxane is placed in contact with DBU for long periods of time.

This set of experiments indicate that decomposition of (1*S*)-(+)-10-camphorsulfonyl chloride is occurring faster than the formation of the sulfonamide on the rotaxane. This is most likely due to the low nucleophilicity of the dibenzylamine in the rotaxane architecture. In light of these results, we abandoned the use of sulfonamide as a chiral stopper.

3.8 Reaction with camphanyl chloride

In a second instance, (1*S*)-(-)-camphanyl moiety was tested as chiral stopper to functionalize the free central amine. The reaction with the rotaxane is, therefore, aimed at producing an amide group starting from the amino group. The reaction conditions are very similar to those used for sulfonamide formation. We envisioned that the acyl chloride should display a higher reactivity with the amine than the sulfonyl chloride, being it an “hard” electrophile (figure 25).

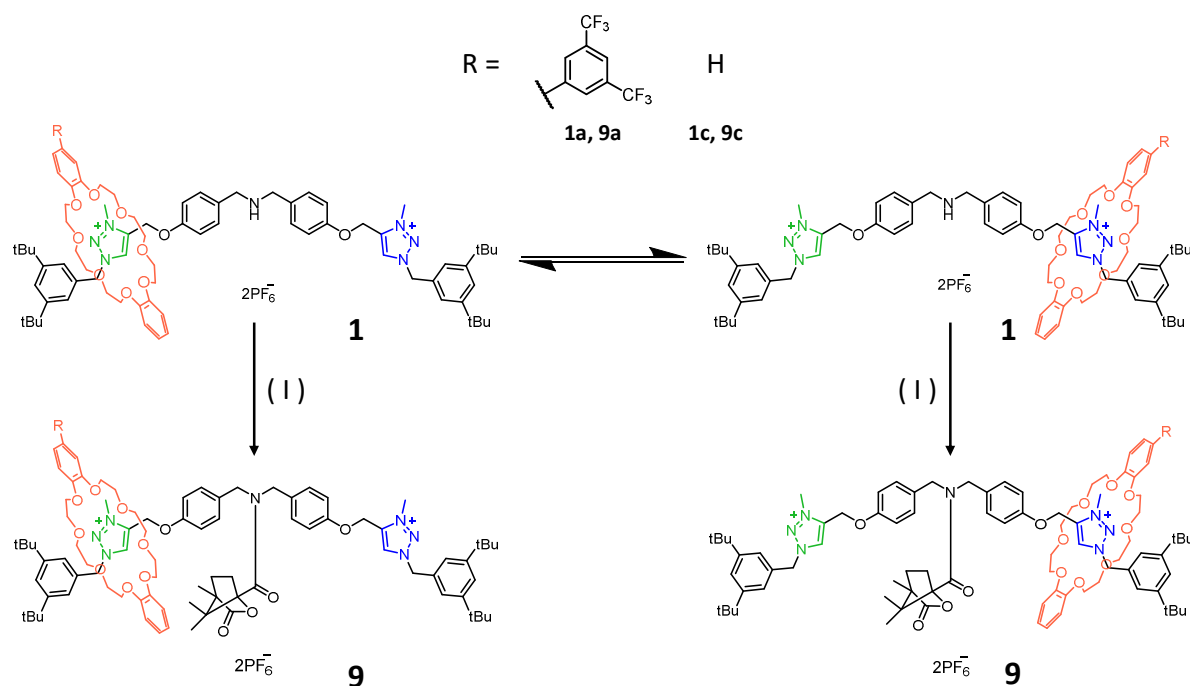


Figure 25. scheme of the reaction between the rotaxanes **1a** and **1c** and (1*S*)-(-)-camphanyl chloride, producing their stoppered form **9a** and **9c**: I) (1*S*)-(-)-camphanyl chloride, triethylamine.

As previously mentioned, the final product of this reaction is a rotaxane bearing tertiary amide moiety, which exists as two distinct *E* and *Z* isomers in slow exchange on the NMR timescale due to the restricted rotation about the C-N bond because of its partial double bond character.³³ The presence of distinct configurational isomers arising from the presence of central amide groups in rotaxanes was previously reported by the group and it was confirmed that the relative position of the amidic substituent and the macrocycle – respectively pointing “toward” or “away from” the macrocycle – produced two distinct stereoisomers.³⁴ It is, thus, expected that all the resonances double due to the presence of the mixture of *E* and *Z* isomers. In particular, for an achiral rotaxane, four singlets in the region of the triazolium protons between 8 and 9 ppm are expected. Even though the presence of configurational isomers complicates the analysis of the ¹H NMR spectra, it does not affect the kinetic resolution procedure and objective.

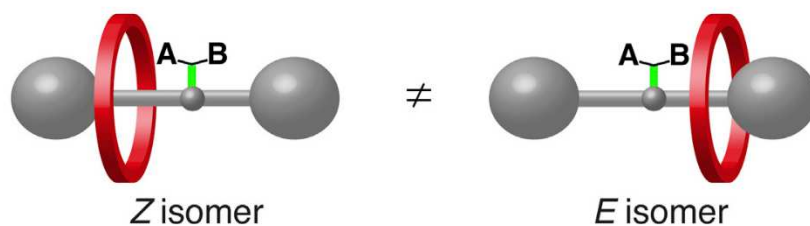


Figure 26. schematic representation of the two configurational isomers *E* and *Z* arising from the CN-CO bond rotation of the tertiary amide moiety embedded in a rotaxane structure.

Also in this case, a reactivity test was first performed using the deprotonated symmetric rotaxane and camphanyl chloride. Exploiting conditions previously optimized in the group for similar reactions, an excess of triethylamine was used as the base. Again, the reaction was performed directly in the NMR tube to facilitate the subsequent ^1H NMR analysis (Figure 27). It is noteworthy that the reaction reached completion within seconds after mixing the reagents.

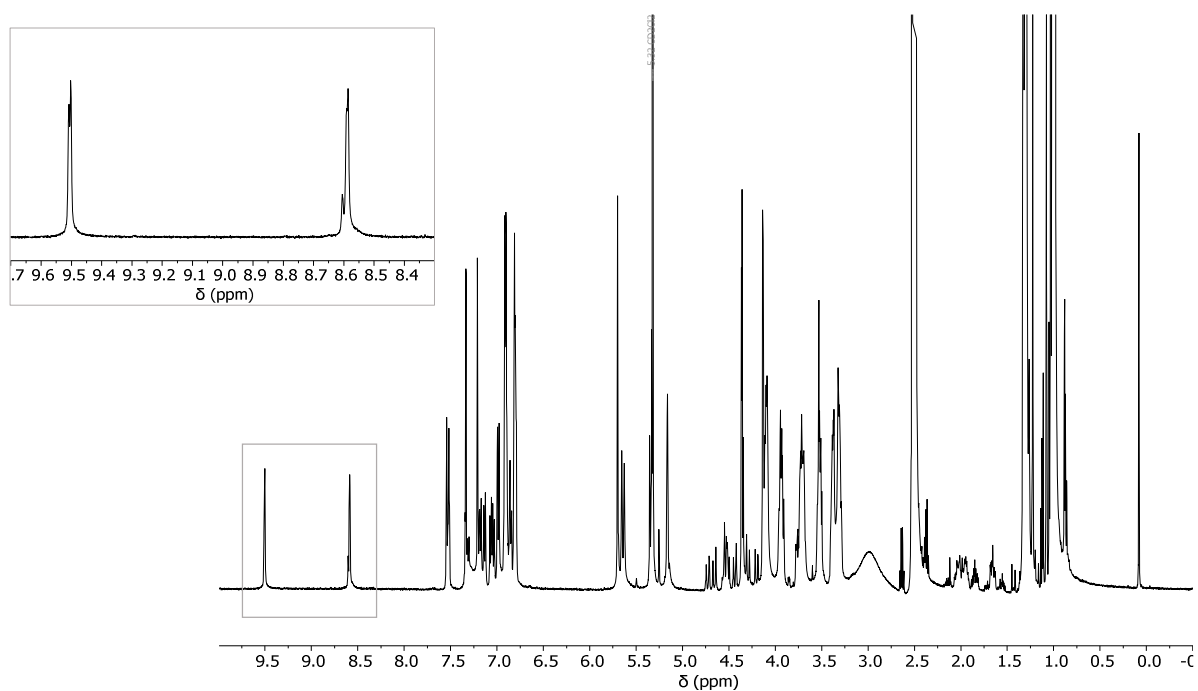


Figure 27. partial ^1H -NMR spectrum (500 MHz, CD_2Cl_2 , 298 K) of the reaction mixture of the achiral rotaxane **1c** with the (1*S*)-(-)-camphanyl chloride. Top left: the portion of the spectrum between 8.5 and 9.5 ppm showing the signals of the complexed and free triazolium unit respectively.

The ^1H NMR spectrum, in the region of the triazolium protons, clearly displays two sets of signals corresponding respectively to the free and complexed triazolium stations. Moreover, they resonate as two sharp singlets indicating that the shuttling is slow on the NMR timescale,

as expected from a stoppering reaction. It can be also noticed that each set of signals is split into two peaks, for a total of four signals, confirming the presence of the distinct *E* and *Z* species. Considering these promising results, reactivity experiments were performed with mechanically planar chiral rotaxane **1a**. Rotaxane **1a** was treated with (1*S*)-(-)-camphanyl chloride under the conditions optimized with the symmetric rotaxane **1c**. Also in this case amide formation occurred within seconds and the reaction mixture was analysed by ¹H NMR.

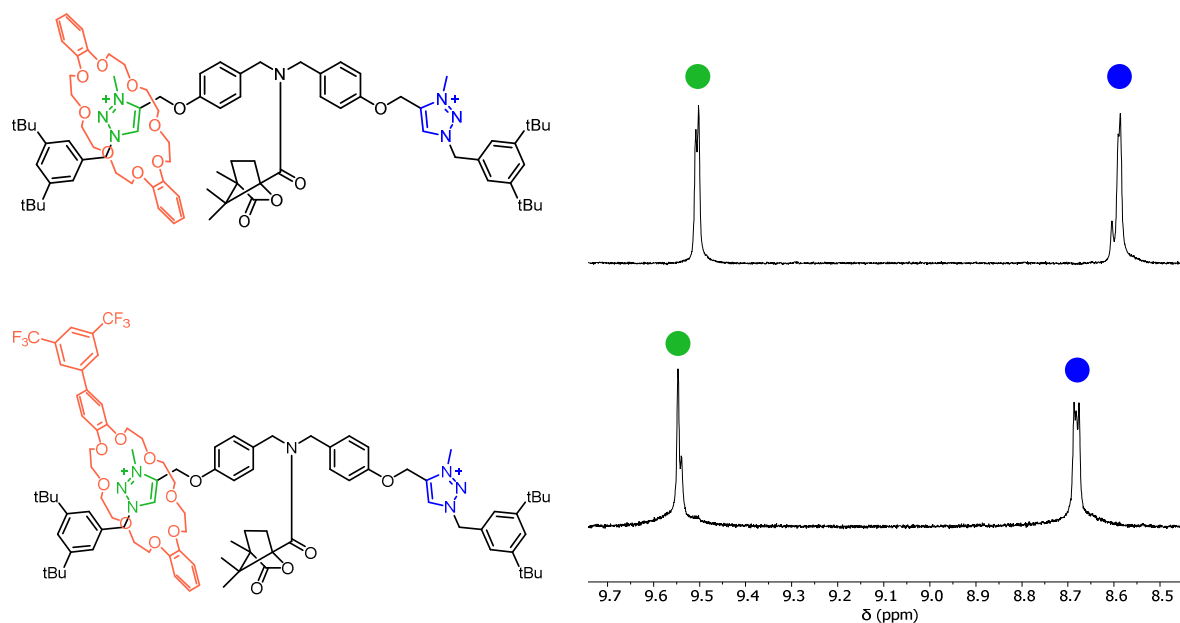


Figure 28. partial ¹H NMR spectra of the rotaxanes **9c** and **9a** (from top to bottom, 500 MHz, CD₂Cl₂, 298 K) around the complexed (green) and free (blue). The rotaxane **9a** displays a more complex signal structure, suggesting the presence of structures other than the configurational isomers. Only one stereoisomer of **9a** is depicted for clarity.

The resulting ¹H NMR spectrum shows a several signals, with the free and complexed triazolium protons appearing as composed sets of signals with multiple overlapped singlets, with a pattern substantially more complex than that observed for the symmetric model rotaxane **1c**. This constitutes important evidence of the presence of multiple stereoisomers including, but not limited to, the *E* and *Z* isomers. Theoretically, in fact, a mechanically planar chiral rotaxane stoppered with an optically pure chiral stopper contains two stereogenic elements, thus, it can exist in four different diastereomers arising from all the possible combinations of the mechanically planar and the point chirality. These are pairs of enantiomers, therefore only two distinct diastereomers could be distinguishable by NMR. As a result, we expect that the each diastereomer display distinct singlets for the free and complexed triazolium stations, that is in

total four signals. On top of that, in the presence of distinct configurational isomers each diastereomer can exist in the *E* and *Z* configuration. Therefore, each of the expected four signals can potentially be divided into two distinct singlets corresponding to the *E* and *Z* configured amide bond. In total, the two triazolium characteristic signals for each stereoisomer can appear as up to eight singlets (figure 29).

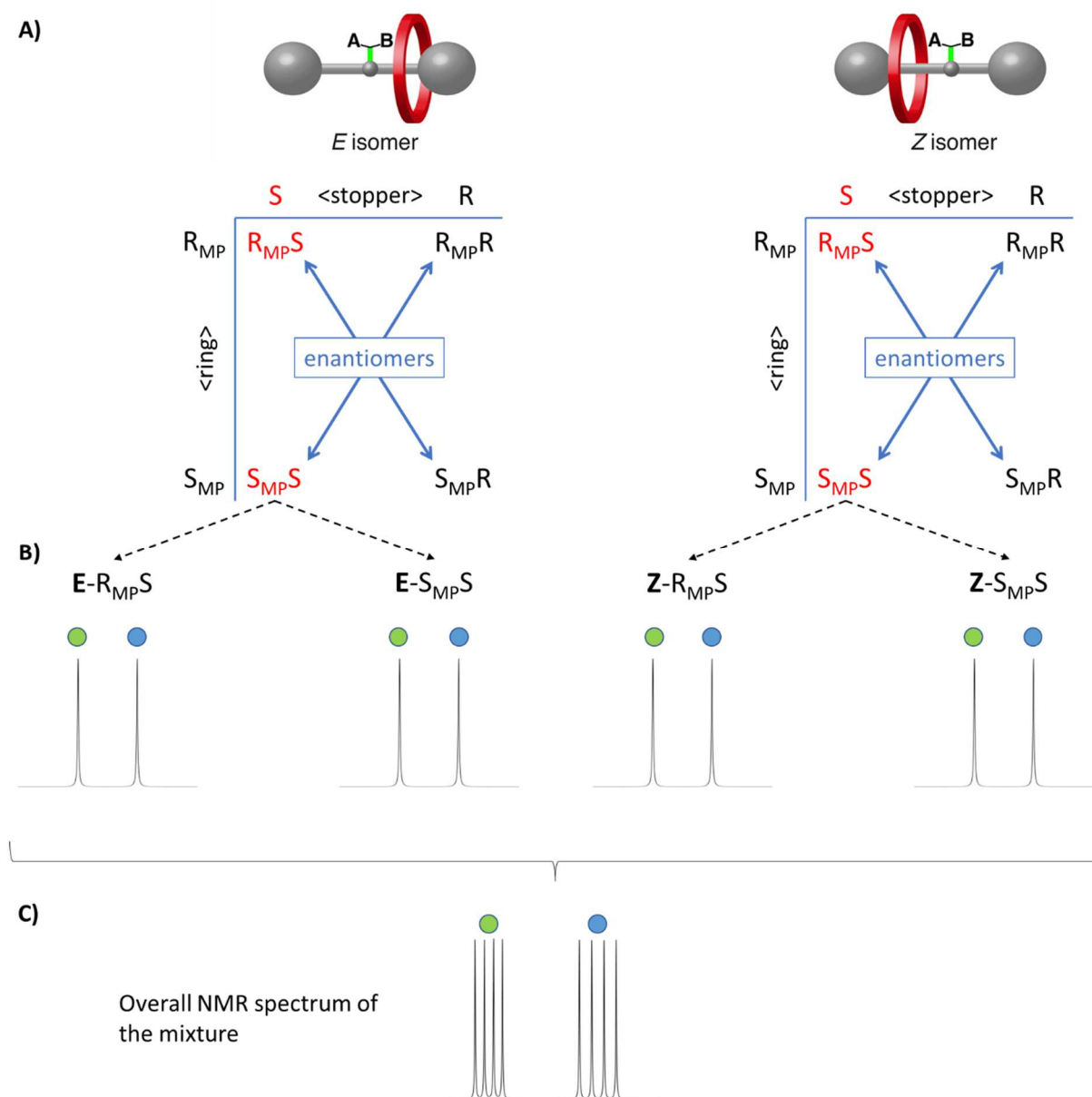


Figure 29. conceptual deconvolution of the ^1H NMR signal of the complexed (green) and free (blue) triazolium station: A) scheme representing all possible diastereomers derived from the CN-CO bond configuration (*E* and *Z*), the point chirality of the camphanyl group (*S* and *R*) and the mechanically planar chirality (R_{MP} and S_{MP}). The stereoisomers effectively present in the mixture are marked in red. B) Expected signal pattern for the complexed and uncomplexed triazolium for each stereoisomer. C) Overall expected NMR signal pattern for the complexed and uncomplexed triazolium in the mixture of the four stereoisomers.

In order to gain a deeper insight in the nature of the signals, variable temperature (VT) NMR experiment was performed. Spectra of the reaction mixture in CD_2Cl_2 were acquired at different temperatures ranging from 233 K to 303 K every 10 K. VT-NMR experiments were also performed in different solvents in order to access a larger temperature range – due to a more favourable boiling point – and to obtain a better resolution of the peaks. The solvent itself, in fact, greatly affects the shape of the peaks due to its polarity and interaction with the compounds. We chose deuterated acetonitrile, that gives access to a wider temperature range (238 K – 358 K) and deuterated DMSO, which proved beneficial to enhance signals resolution.

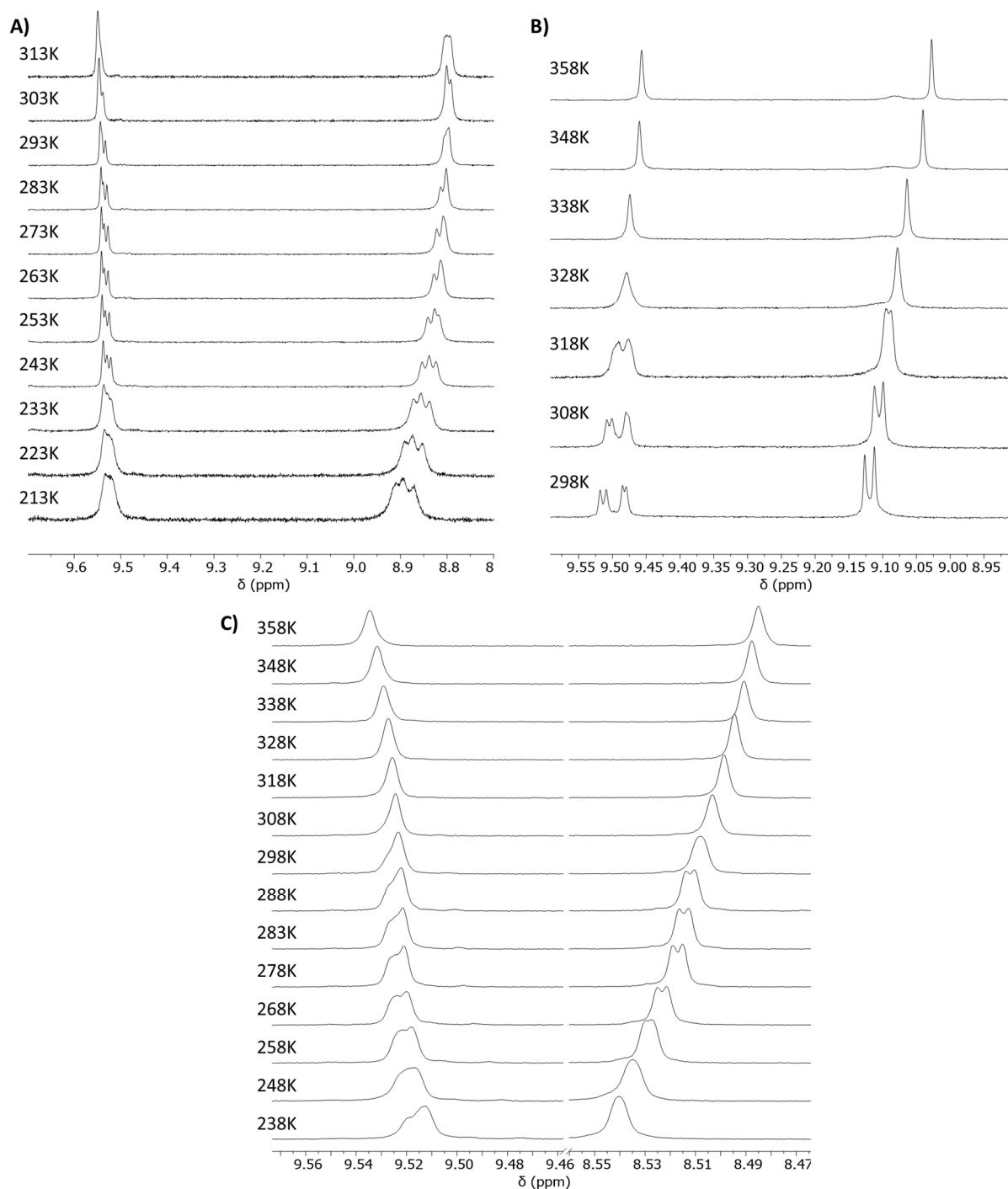


Figure 30. VT-NMR spectra (500 MHz) of the rotaxane **9a** in the region of the triazolium signals, in different solvents: A) CD_2Cl_2 ; B) d -DMSO; C) CD_3CN .

To our pleasure, the signals nicely separated at different temperatures or in different solvents. In particular, we focused our attention on the signals corresponding to the protons of the encircled triazolium. In CD_2Cl_2 at 243 K and in DMSO at 298 K these are clearly visible as a set of four distinct resonances (Figure 30). These observations are perfectly in line with the presence of two different diastereomers each displaying *E* or *Z* configuration of the C-N amide

bond. Similar observations could be made for the set of signals corresponding to the free triazolium protons, which however display a much larger degree of overlap of the diastereomeric signals (Figure 30) possibly due to the distance from the mechanically planar stereogenic unit which formally resides on the macrocycle plane. Finally, comparison with the symmetric rotaxane **1c**, displaying only configurational isomerism, in DMSO also confirmed the presence of two signals for both complexed and uncomplexed triazolium protons, corresponding to the *E*- and *Z*-configured amide bond (Figure 31).

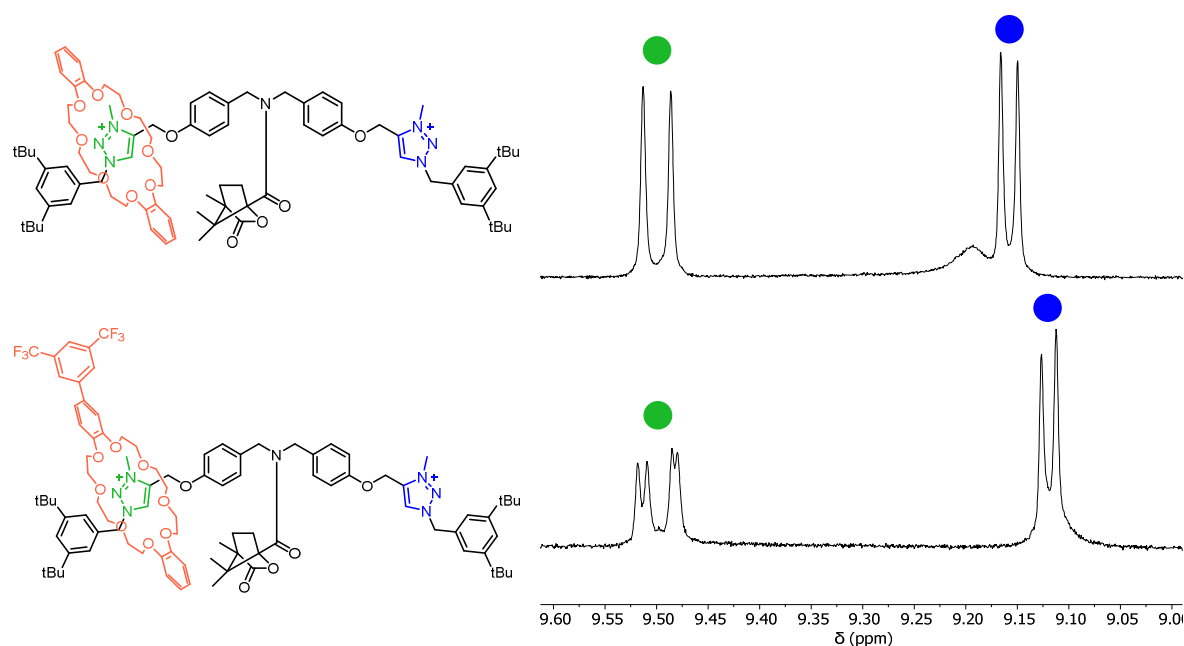


Figure 31. partial ^1H NMR spectra (500 MHz, *d*-DMSO, 298 K) of rotaxanes **9c** (top) and **9a** (bottom) displaying signals of the free (blue) and complexed (green) triazolium stations. The appearance of two additional signals in the complexed triazolium unit for rotaxane **9a** is clearly visible, indicating the presence of two diastereomers together with the configurational isomers. Only one stereoisomer of **9a** is depicted for clarity.

Spectra were recorded at higher temperatures in DMSO in order to increase the CN-CO bond rotation rate until it became fast on the NMR timescale, giving rise to a single set of signals for the *E* and *Z* isomers. This was done with the dual aim of simplifying signal analysis and univocally identify the signals belonging to the configurational isomers and those of the diastereomers. Unfortunately, the loss in resolution upon increasing the temperature was such that no clear distinction of the peaks was possible. Nonetheless, spectra recorded in DMSO in the intermediate rate range (308 K and 318 K) suggest that it the isomers start coalescing while the diastereomers do not (Figure 30, B). This is expected since ring shuttling is completely

inhibited by the presence of the stopper, while amide bond rotation can occur and strongly support our hypothesis that these signals belong to the four aforementioned species.

In acetonitrile, conversely, the same signals are present as two partially overlapped broad singlets at all temperatures, (Figure 30, C) and we were unable to fully resolve the signals. From 268 to 283 K the same pattern of four overlapping broad singlets can be recognized, however, at higher and lower temperatures, the signals coalesced forming one broad singlet.

Interestingly, the greater difference in chemical shift is recorded for the signals of the configurational isomers and not the diastereomers. This is somewhat expected considering the peculiar nature of chirality displayed structure displayed by mechanically planar chiral rotaxanes. In particular, a very small difference in chemical environment, and thus in NMR chemical shift, is expected for these diastereomers considering their three-dimensional structure. Thanks to the presence of fluorine atoms in the macrocycle, ^{19}F NMR spectra were recorded along with the proton spectra. The macrocycle CF_3 groups resonate as a single signal in the case of a deprotonated rotaxane and should present multiple signals for the diastereomeric rotaxane arising from the presence of different stereoisomers in the same way as the proton spectrum. In the recorded spectra, multiple overlapped signals can be seen at certain temperatures in both CD_3CN and DMSO but it is hard to extract reliable data from these results. Nonetheless, they provide additional evidence of the presence of different stereoisomers.

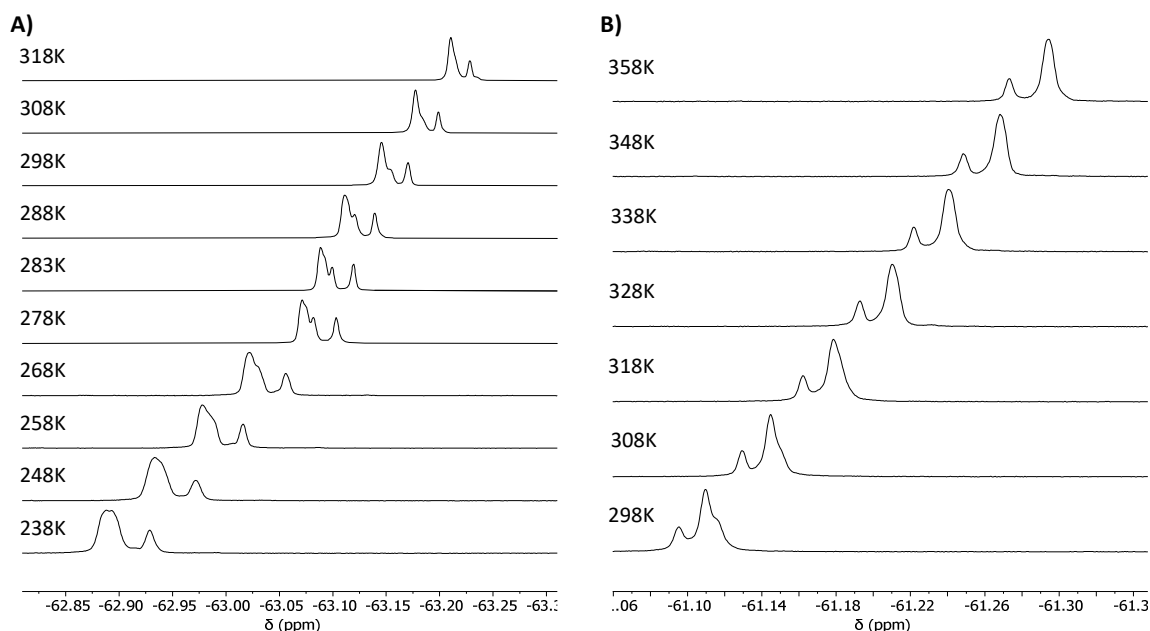


Figure 32. partial ^{19}F NMR spectra (470 MHz) at different temperatures of the rotaxane **9a** showing the signals associated with the $-\text{CF}_3$ moieties of the macrocycle in CD_3CN (A) and DMSO (B).

4. CONCLUSIONS

In this thesis, two prochiral asymmetric rotaxanes, along with a symmetric model rotaxane, were prepared through a previously optimized multistep route. The key step of the synthesis involves the stoppering of a self-assembled pseudo-rotaxane complex between a dibenzo-24-crown-8 (DB24C8) ether-type ring and a dibenzylammonium axle. The stoppering reaction was performed by Cu(I)-catalysed azide-alkyne cycloaddition. Both rotaxanes encompass an axle component with identical extremities. An ammonium station is installed, for synthetic purposes, at the centre of the axle, flanked by two equivalent, weak, triazolium stations. These can host the macrocycle upon deprotonation/deactivation of the ammonium station.

The two rotaxanes differ over the choice of the oriented macrocycle, one bearing a 3,5-ditrifluoromethylphenyl (ring **A**) and one with a dimethyl-*t*-butyl alkyne moiety (ring **B**).

The two functionalised DB24C8 crown ethers **A** and **B** were selected to take advantage of their peculiar properties, such as the presence of fluorine nuclei detectable by ^{19}F NMR and the presence characteristic diastereotopic CH_3 signals at high fields, that is region of the ^1H NMR spectrum free of other, interfering, signals.

The rotaxanes were first characterized via NMR spectroscopy in the prochiral form. Then, the ammonium was deprotonated in order to switch on the shuttling movement between the two equivalent triazolium stations and the MP chirality. The MP chiral rotaxanes were also characterized by ^1H NMR spectroscopy confirming the fast interconversion, on the NMR timescale, between two equivalent co-conformations.

A dynamic kinetic resolution of the two MP enantiomers was attempted on rotaxane **1a** using two optically pure reagents to functionalize the central amine moiety: (1*S*)-(+)-10-camphorsulfonyl chloride and (1*S*)-(-)-camphanyl chloride. The introduction of a bulky group in the centre was expected to inhibit the shuttling “blocking” the ring on one side of the axle. Moreover, the use point chirality on the stopper was expected to bias the shuttling equilibrium toward one MP enantiomer and to form two diastereomers and distinguish them by ^1H NMR. The reaction with the camphorsulfonyl chloride to produce a sulphonamide failed as the sulfonyl chloride hydrolysed quickly even in presence of traces of water. Conversely, the reaction with the acyl chloride was successful, providing full conversion within minutes after

optimization. The stoppering effect of the amide substituent was clear from the presence of distinct, sharp signals associated with the complexed and uncomplexed triazolium stations.

As expected, the addition of an optically pure stopper to the central amine station produced four different stereoisomers overall. Two diastereomers arise from the presence of MP and point stereogenic elements, while two configurational isomers are due to the slow rotation about the CN-CO bond of the amide moiety.

Each of these stereoisomers produces its own set of signals in the $^1\text{H-NMR}$ spectrum, with an expected total of four resonances for each magnetically different proton.

Upon optimization of the conditions, the best combination of temperature and solvent for the NMR analysis were found. All four stereoisomers could be identified through careful analysis of the characteristic singlets associated with the complexed triazolium, which are sharp and isolated. Comparison of the spectra with those of a rotaxane stoppered with the same reaction conditions that do not exhibit MP chirality, allowed to characterize the configurational isomers and distinguish their signals from the diastereomers.

Ultimately, this set of results proves the presence of a mechanically planar stereogenic element in the synthesized rotaxane, where the position of an oriented macrocycle along the axle produces diastereomers in correlation with point chirality.

However, at this stage the reaction performed with an enantiopure reagent produced both diastereomers in an equal amount. Therefore, future efforts will be devoted to achieving a kinetic resolution of the MP chiral rotaxane and the preferential synthesis of one diastereomer over the other. One way to reach an enantiomeric excess could be performing the reaction at lower temperatures, in order to increase enantioselectivity of the stoppering reaction.

5. EXPERIMENTAL SECTION

Materials

Solvents and reagents were all used as supplied by Fluorochem, Sigma-Aldrich or VWR and used as received. All procedures were carried out in air unless otherwise specified. Flash column chromatography was performed using Sigma Aldrich Silica 40 (230-400 mesh size or 40-63 μm) as the stationary phase. Thin layer chromatography was performed on TLC Silica gel 60 F254 coated aluminium plates from Merck. Size exclusion chromatography was performed using Biorad Biobeads SX-1 or SX-3 as stationary phase and CH_2Cl_2 as eluent.

Instruments and methods

The ^1H , ^{19}F and ^{13}C NMR spectra were recorded at 298 K in deuterated solvents (from Cambridge Isotope Laboratories, Inc.) by using either a Varian DD3 500 MHz spectrometer or a Varian Mercury 400 MHz spectrometer. Chemical shifts (δ) are quoted in ppm using the residual solvent signal as the internal standard. Coupling constants (J) are expressed in Hertz (Hz).

5.1 Synthesis of the oriented crown ethers

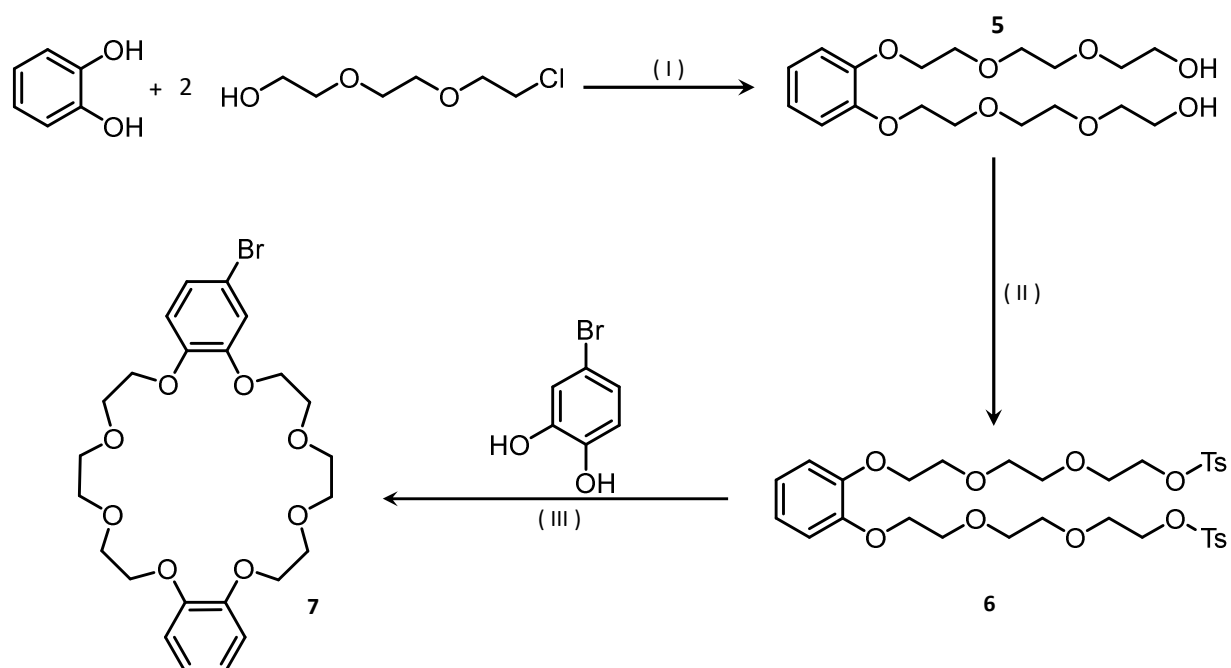


Figure 33. Synthetic route to the compound 7. I) K_2CO_3 , ACN dry, N_2 reflux 48h; II) Et_3N , TsCl, cat. DMAP, N_2 , $0^\circ C$, 72h; III) Cs_2CO_3 , THF dry, N_2 atmosphere, reflux, 24h.

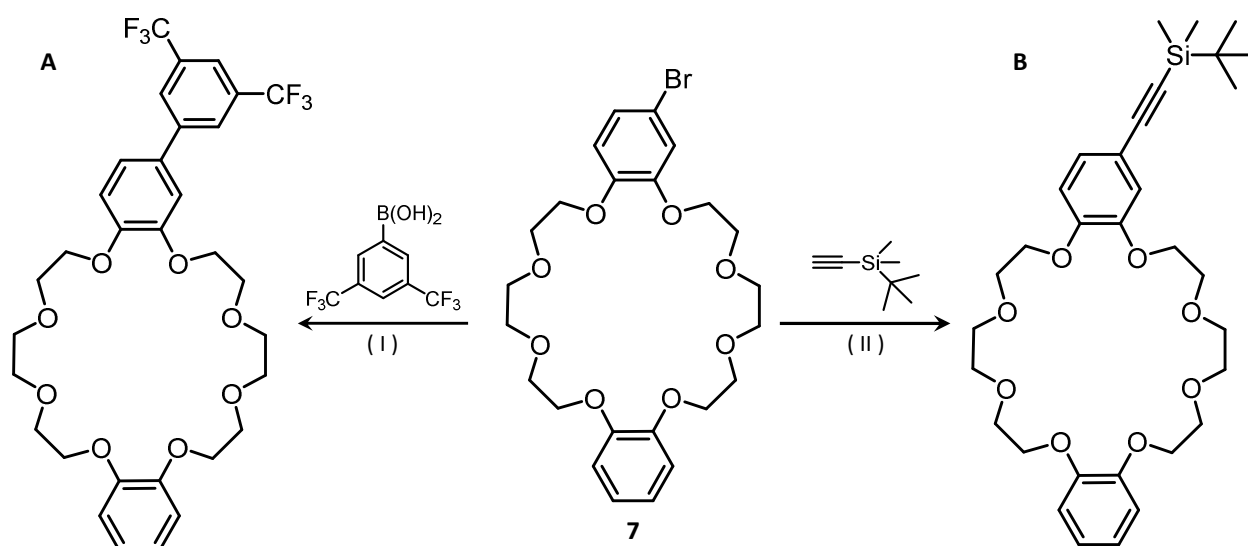
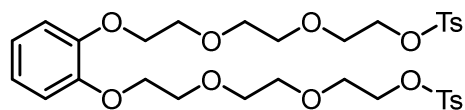


Figure 34. Synthetic route to the compounds A and B. I) $Pd(PPh_3)_4$, K_2CO_3 ; II) $Pd(PPh_3)_4$, CuI, DMF, Diisopropylamine, $85^\circ C$, N_2 atmosphere, reflux.

Compound 6



To a solution of catechol (6.5 g, 59 mmol) in dry acetonitrile under a N₂ atmosphere, was added K₂CO₃ (20.4 g, 147 mmol). The suspension was heated to reflux under stirring. A solution of Triethylene glycol monochlorohydrin (21.89 g, 130 mmol) was added to the reaction mixture dropwise over 30 minutes. Stirring is then continued for 2 days, then the mixture was cooled to room temperature. Acetonitrile was removed under vacuum. The crude residue was dissolved in dichloromethane (200 mL) and washed with H₂O (3 x 100 mL). The organic layer was dried over Na₂SO₄ and concentrated under vacuum. The product was isolated as a brownish oil and was used without further purification (yield 56%).

The obtained compound **5** (12.46 g, 33.3 mmol) was dissolved in CH₂Cl₂ (300 mL) along with triethylamine (46.3 mL, 333 mmol) and the DMAP catalyst (400 mg, 3.3 mmol). The mixture was cooled to 0 °C under a N₂ atmosphere. A solution of p-toluenesulfonyl chloride in CH₂Cl₂ (200 mL) was slowly added to the reaction mixture.

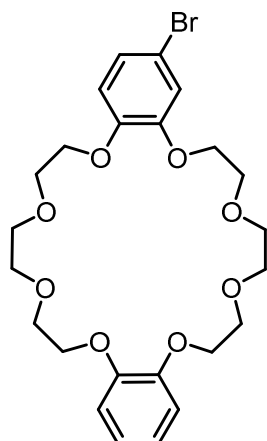
Upon completing the addition, the reaction mixture was stirred at room temperature for 72 hours. The formation of the product was monitored by TLC (SiO₂, CH₂Cl₂/MeOH 95:5).

The reaction mixture was then washed with HCl 1M (2 x 500 mL) and brine (2 x 500 mL) and dried over Na₂SO₄. The solvent was removed under vacuum and the crude product was purified by column chromatography (SiO₂, hexane/EtOAc 2:1, 1:1, 1:2, 1:4 and then pure EtOAc). Compound **2** was isolated as an orange oil (9.351 g, 13.7 mmol, 41 %).

¹H NMR (500 MHz, CDCl₃, 298 K) δ 7.64 (d, 4H), 7.19 (d, *J* = 8.2 Hz, 4H), 6.82 – 6.74 (m, 4H), 4.00 (m, 8H), 3.67 (m, 4H), 3.53 (m, 8H), 3.44 (m, 4H), 2.26 (s, 6H).

¹³C NMR (126 MHz, CDCl₃, 298 K) δ 148.92, 144.81, 132.85, 129.86, 127.77, 121.56, 114.82, 70.54, 69.65, 69.45, 68.76, 68.48, 21.44.

Compound 7

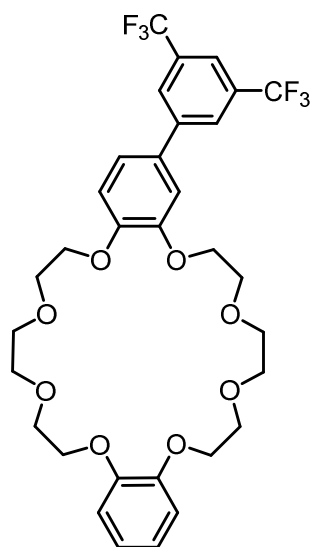


Cs_2CO_3 (1.31 g, 4 mmol) was suspended in 500 mL of THF under a N_2 atmosphere and the suspension was heated to reflux. A solution of 4-bromobenzene-1,2-diol (1.504 g, 8 mmol) and compound **6** (5.504 g, 8 mmol) in 100 mL of acetonitrile was added over 72 h using a dropping funnel directly into the boiling suspension. Afterwards, reflux was continued for 48 h. The reaction was allowed to cool to room temperature and the solvent was removed in vacuo. The residue was dissolved in EtOAc and water. The phases were separated, and the aqueous layer was extracted with EtOAc. The combined organic layers were dried over Na_2SO_4 and the solvent was removed in vacuo. The product was purified by hot filtration: the residue was suspended in cyclohexane and the mixture was heated until the boiling temperature was reached, the non-soluble sticky impurities were filtered into a hot round bottom flask, the solution was left to return to room temperature then the white crystals formed were collected by filtration under vacuum. The product was isolated as colourless powder (2.20 g, 4 mmol) yield 50%.

^1H NMR (500 MHz, CDCl_3 , 298 K) δ 6.99 (dd, $J = 8.5, 2.3$ Hz, 1H), 6.97 (d, $J = 2.2$ Hz, 1H), 6.93 – 6.84 (m, 4H), 6.72 (d, $J = 8.5$ Hz, 1H), 4.13 (dd, $J = 19.5, 4.6$ Hz, 8H), 3.91 (d, $J = 4.5$ Hz, 8H), 3.82 (s, 8H).

^{13}C NMR (126 MHz, CDCl_3 , 298 K) 149.9, 149.0, 148.3, 124.0, 121.6, 117.2, 115.4, 114.2, 113.3, 71.4, 70.0, 69.9, 69.8, 69.7, 69.5.

Compound A



The following solutions were prepared under inert conditions and degassed by bubbling N_2 for half an hour each: compound **7** (1.2 g, 2.3 mmol) in toluene (250 mL); 3,5-Di(trifluoromethyl)benzeneboronic acid (1.5 g, 5.8 mmol) in methanol (20 mL) and aqueous Na_2CO_3 (2M, 100 mL). To the solution of compound **7** was also added $Pd(PPh_3)_4$ in catalytic quantities (180 mg, 0.16 mmol, 7 mol%). The three solutions were then mixed together and left stirring under a N_2 atmosphere and reflux for 48 hours. Subsequent additions of catalyst (2 x 7 mol%) and 3,5-Di(trifluoromethyl)benzeneboronic acid (0.300 g) were also performed.

The aqueous phase was then separated from the organic layer, and the latter was filtered to eliminate the exhaust catalyst and dried over Na_2SO_4 . The toluene was evaporated under vacuum.

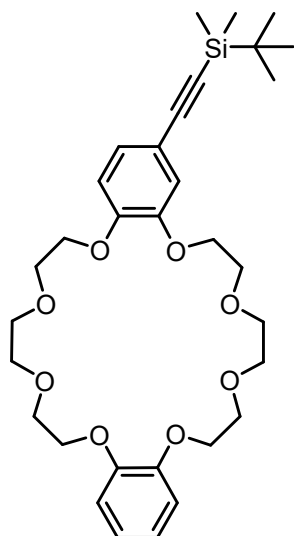
The resulting white powder was dissolved in 400 mL of diethyl ether and washed with an aqueous solution of Na_2CO_3 0.1M (2 x 200 mL) and water (2 x 200 mL). The organic layer was dried over Na_2SO_4 and the solvent was removed under vacuum.

The crude product was purified by column chromatography (SiO_2 , $CH_2Cl_2/MeOH$ 98:2) and precipitation with cold pentane. The product was isolated as a white solid (680 mg, 45% yield).

1H NMR (500 MHz, CD_2Cl_2 , 298 K) δ 8.00 (s, 2H), 7.82 (s, 1H), 7.19 (dd, $J = 8.5, 2.2$ Hz, 1H), 7.14 (d, $J = 2.2$ Hz, 1H), 6.99 (d, $J = 8.3$ Hz, 1H), 6.88 (s, 4H), 4.20 (dt, $J = 16.0, 4.4$ Hz, 4H), 4.11 (t, $J = 4.1$ Hz, 4H), 3.92 – 3.83 (m, 8H), 3.77 (s, 8H).

^{13}C NMR (126 MHz, CD_2Cl_2) δ 150.3, 149.8, 149.4, 143.4, 132.2, 132, 131.6, 127.2, 121.7, 120.7, 114.7, 113.6, 71.5, 70.1 (d, $J = 22.0$ Hz), 69.8 – 69.5 (m).

Compound B



Compound **7** (2 mmol) was added to a 100 ml Shlenk flask with CuI (36 mg, 0.2 mmol, 0.1 equiv.) and Pd(PPh₃)₄ (11 mg, 9.5 μmol, 0.005 equiv.). Diisopropylamine (20mL) was charged under nitrogen and the mixture was degassed for 3 times by a freeze-pump-thaw procedure. (dimethylphenylsilyl)acetylene (550 mg, 5 mmol, 2.5 equiv.) was added *via* syringe. The reaction was stirred at reflux under N₂ flux and the formation of the product was monitored by ¹H-NMR. After completed reactions, the mixture was filtered through a celite plug and the filtrate was concentrated. The compound was then purified through silica gel column chromatography (eluent mixture from EtOAc: *n*-hexane 2:1, to 1:1).

¹H NMR (500 MHz, CDCl₃, 298 K) δ 7.04 (dd, *J* = 8.3, 1.9 Hz, 1H), 6.94 (d, *J* = 1.9 Hz, 1H), 6.92 – 6.84 (m, 4H), 6.75 (d, *J* = 8.3 Hz, 1H), 4.14 (m, *J* = 6.3, 5.1 Hz, 8H), 3.94 – 3.87 (m, 8H), 3.82 (s, 8H), 0.98 (s, 9H), 0.16 (s, 6H).

¹³C NMR (126 MHz, CDCl₃, 298 K) δ 149.67, 149.05 148.41, 125.99, 121.54 117.22, 115.98, 114.20, 113.26, 105.91, 90.81, 71.45 70.05, 69.88, 69.51, 26.29.

5.2 Synthesis of the asymmetric rotaxanes

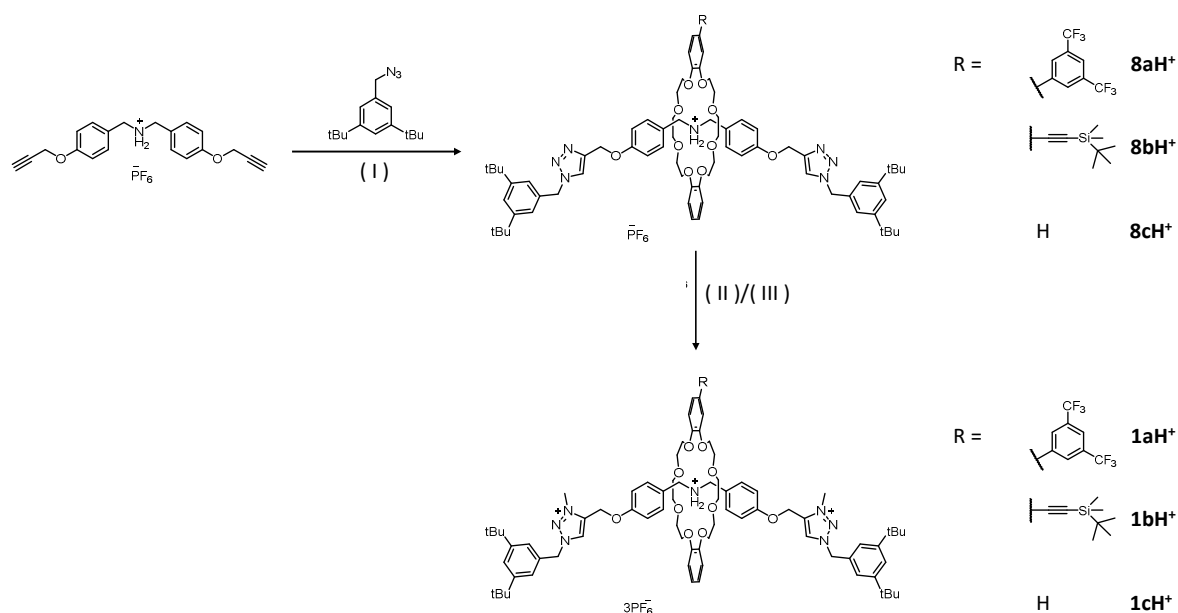


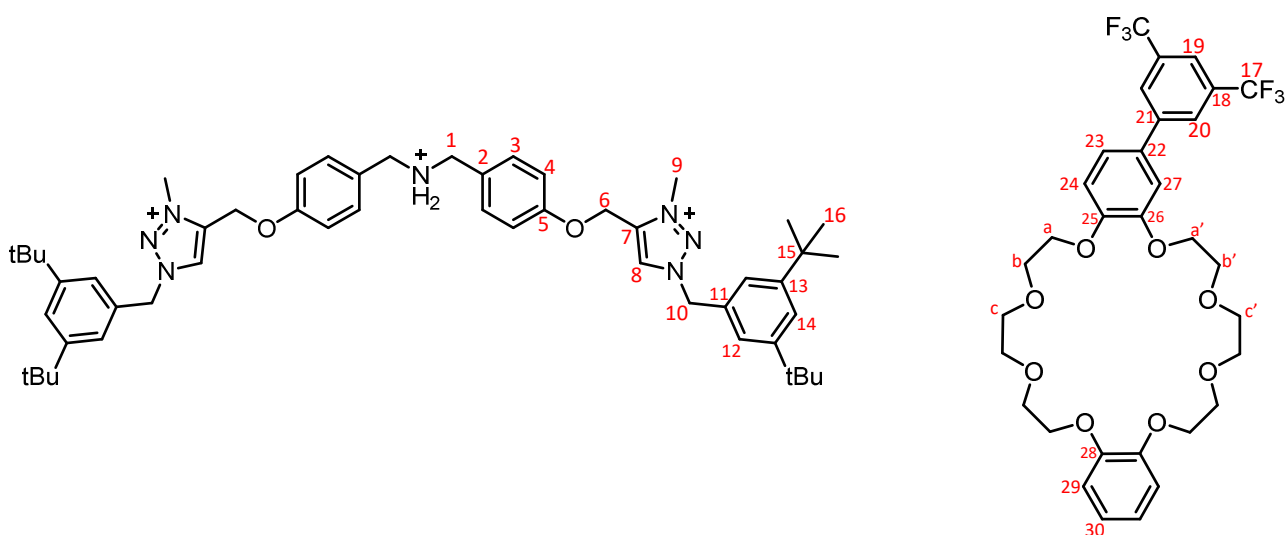
Figure 35. Synthetic route to the compounds $\mathbf{1aH}^+$ and $\mathbf{1bH}^+$. I) $[\text{Cu}(\text{CH}_3\text{CN})_4]\text{PF}_6$, 1-(azidomethyl)-3,5-di-tert-butylbenzene, DB24C8-type macrocycle (**A**, **B** or **C**), DCM 60%; II) 1) CH_3I 2) NH_4PF_6 , DCM; III) 1) MeOt , N_2 , 0°C 2) NH_4PF_6 , DCM.

General protocol for the synthesis of compounds $\mathbf{8aH}^+$ and $\mathbf{8bH}^+$ (**X** = **A**, **B**)

Compound **1a** (1 equiv.) and **X** (2 equiv.) were dissolved in 100 mL of degassed CH_2Cl_2 and stirred under a N_2 atmosphere for 3 hours. 3,5-di-(tert-butyl)benzyl azide (2 eq) and $\text{Cu}(\text{CH}_3\text{CN})_4\text{PF}_6$ (0.8 eq) were then added to the mixture and stirring continued for one week. The mixture was diluted with CH_2Cl_2 and washed with EDTA (0.1 M) and water. The organic layer was dried over Na_2SO_4 and the solvent was removed under vacuum. The crude product was then purified through size-exclusion chromatography (biobeads SX-3 resin, CH_2Cl_2).

Compound 1aH⁺

Compound **8aH⁺** (200 mg, 0.08 mmol) was dissolved in anhydrous CH₂Cl₂ (20 mL) at 0°C and under N₂ atmosphere. Methyl triflate (23 μL, 0.2 mmol) was then added via Hamilton syringe through a sealed septum. The reaction was left stirring for 1 hour. The crude product was diluted with additional 30 mL of CH₂Cl₂ and washed with NH₄PF₆ (2 x 50 mL) and water (2 x 50 mL). The organic layer was then dried over Na₂SO₄ and the solvent was removed under vacuum. The crude compound was purified by size exclusion chromatography (Biobeads SX-300 resin, CH₂Cl₂) and the desired compound was isolated as a white glassy solid (yield 80%).



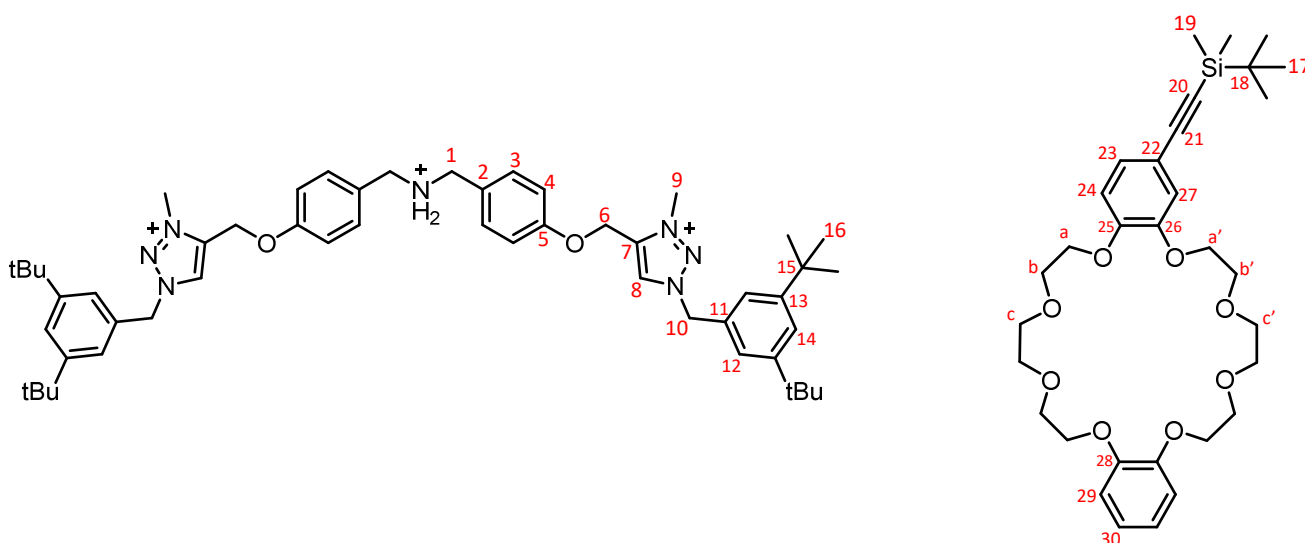
¹H NMR (500 MHz, CDCl₃, 298 K) δ 8.39 (s, 2H, **8**), 7.95 (s, 2H, **20**), 7.83 (s, 1H, **19**), 7.57 (br., 2H, -NH₂) 7.54 (s, 2H, **14**), 7.32 (m, 8H, **3,12**), 7.19 (dd, J = 8.4, 2.0 Hz, 1H, **23**), 7.02 (d, J = 1.9 Hz, 1H, **27**), 6.99 (d, J = 8.5 Hz, 1H, **24**)., 6.85 (m, 6H, **4, 29**), 6.76 (m, 2H, **30**), 5.66 (s, 4H, **10**), 5.20 (s, 4H, **6**), 4.63 – 4.54 (m, 4H, **1**), 4.31 (s, 6H, **9**), 4.21 (t, J = 5.5 Hz, 4H, **a'**), 4.09 – 4.00 (m, 4H, **a**), 3.88 (d, J = 6.0 Hz, 4H, **b'**), 3.72 (m, 4H, **b**), 3.56 (m, 8H, **c, c'**), 1.32 (s, 36H, **16**).

¹³C NMR (126 MHz, CD₂Cl₂, 298 K) δ 157.9 (**5**), 153.3 (**28**), 149.1 (**15**), 148.8 (**26**), 147.7 (**25**), 147.8 (**11**), 143.3 (**21**), 140.3 (**7**), 132.2 (**22**), 132.1 (q, J= 28.0 Hz, **17**), 132.0 (**29**), 131.7 (**3**), 129.7 (**8**), 127.4 (**20**), 126.4 (**2**), 125.2 (**14**), 124.4 (**12**), 122.1 (**30**), 122.0 (**23**), 121.1 (**19**),

115.3 (4), 113.8 (24), 112.0 (27), 71.4/71.3/70.9/70.7 (c, c'), 69.0 (b, b'), 68.7 (a, a'), 59.4 (6), 58.5 (10), 52.4 (1), 39.4 (9), 35.4 (13), 31.5 (16).

Compound **1bH**⁺

Compound **8bH**⁺ (100 mg, 0.065 mmol) was dissolved in iodomethane (6 mL) and the mixture was stirred at room temperature for 72 hours. Volatiles were removed with a stream of N₂ and the residue was dissolved in CH₂Cl₂ (100 mL). The solution was then washed with aqueous NH₄PF₆ (3 x 100 mL). The organic layer was dried over Na₂SO₄ and concentrated under reduced pressure. The crude compound was purified by size exclusion chromatography (Biobeads SX-300 resin, CH₂Cl₂) to afford **1bH**⁺ as an off-white glassy solid (41 mg, 0.023 mmol, yield: 35 %).



¹H NMR (500 MHz, CDCl₃, 298 K) δ 8.40 (s, 2H, 8), 7.95 (s, 2H, 20), 7.83 (s, 1H, 19), 7.57 (br., 2H, -NH₂) 7.55 (s, 2H, 14), 7.31 (m, 8H, 3,12), 6.85 (m, 6H, 4), 7.15 – 6.70 (m, 7H, 23, 24, 27, 29, 30) 5.67 (s, 4H, 10), 5.22 (s, 4H, 6), 4.56 (m, 4H, 1), 4.34 (s, 6H, 9), 4.20 – 3.45 (m, 24H, a', a, b', b, c, c'), 1.35 (s, 36H, 16), 0.96 (s, 9H, 17), 0.14 (s, 6H, 19).

¹³C NMR (126 MHz, CD₂Cl₂, 298 K) δ 157.8 (5), 153.2 (15), (26), (25), 122.9 (11), (21), 140.2 (7), (22), 131.5 (3), 129.7 (8), 126.2 (2), 125.0 (14), 124.2 (12), 122.4 – 112.0 (23, 24, 27, 28,

29, 30), 121.1 (19), 115.1 (4), 91.7 (20), 72.5 – 67.5 (c, c', b, b', a, a'), 58.4 (6), 59.2 (10), 52.3 (1), 39.3 (9), 35.2 (13), 31.4 (16), 16.9 (18).

General procedure for the synthesis of compound 9a

5 mg of compound **1a** (1.37 μmol) were dissolved in 0.5 mL of CD_2Cl_2 inside an NMR tube together with 1.9 μL of anhydrous triethylamine (1.37 μmol , 10 eq).

Afterwards, 8.6 μL of (1*S*)-(-)-camphanyl chloride (0.16 M, 1.37 μmol) were added to the reaction mixture. After a few minutes, the reaction mixture was analysed at the NMR.

^1H NMR and ^{13}C NMR spectra of compound 6

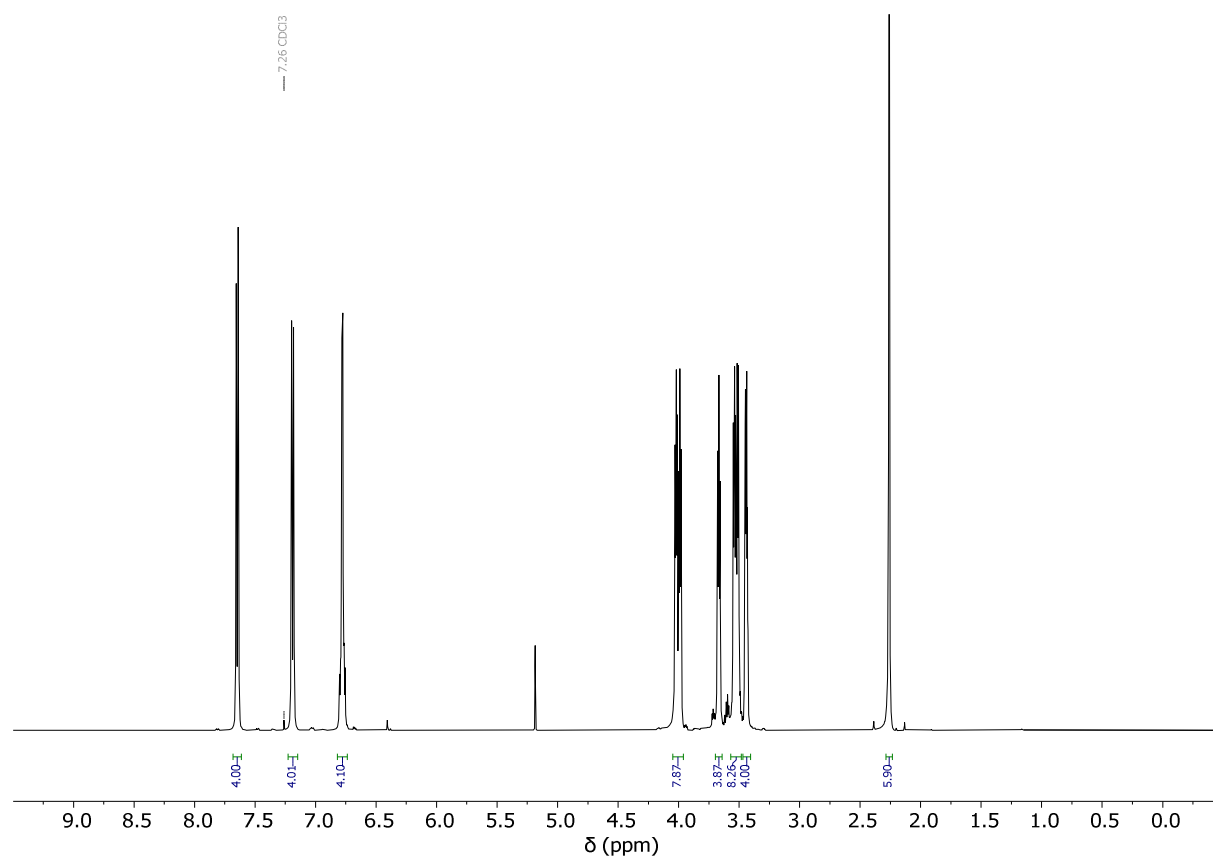


Figure 36. ^1H NMR spectrum of compound 6 (500 MHz, CDCl_3 , 298K)

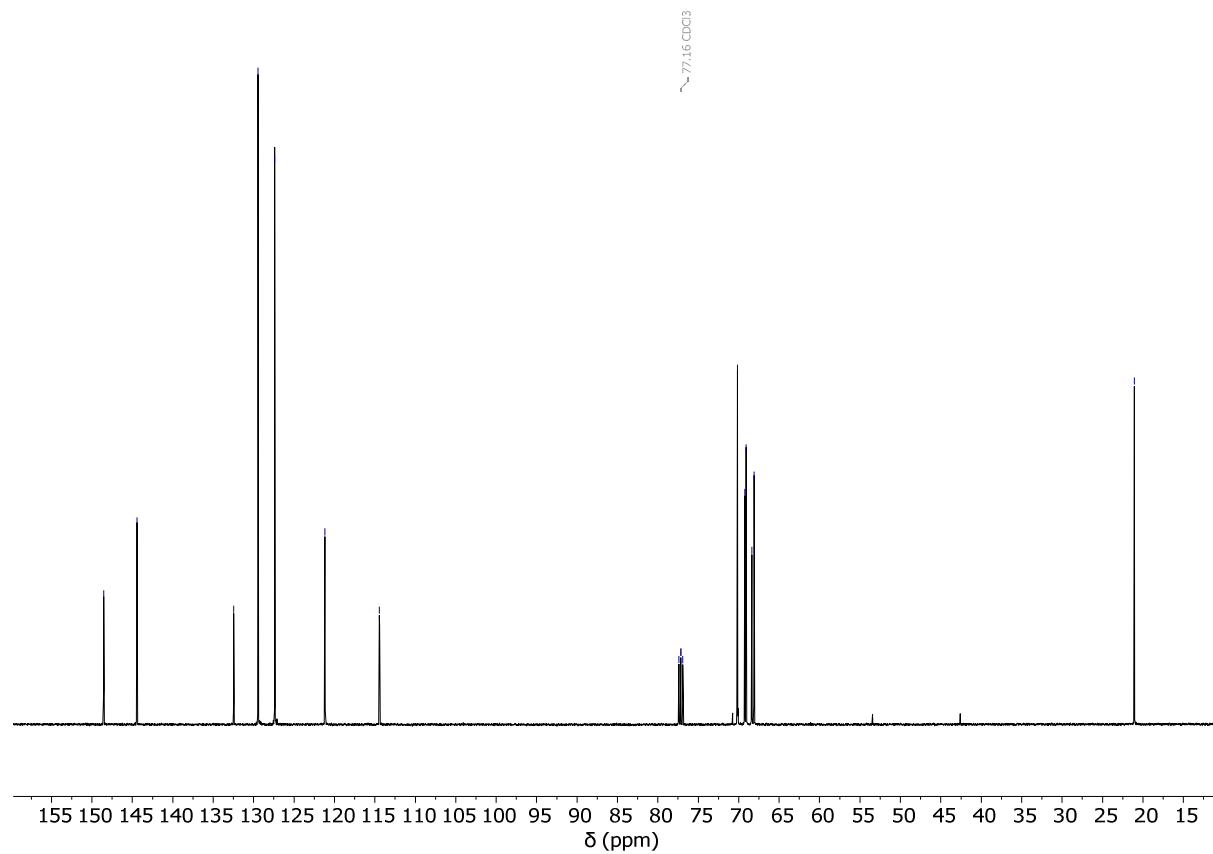


Figure 37. ^{13}C NMR spectrum of compound 6 (126 MHz, CDCl_3 , 298K)

^1H NMR and ^{13}C NMR spectra of compound 7

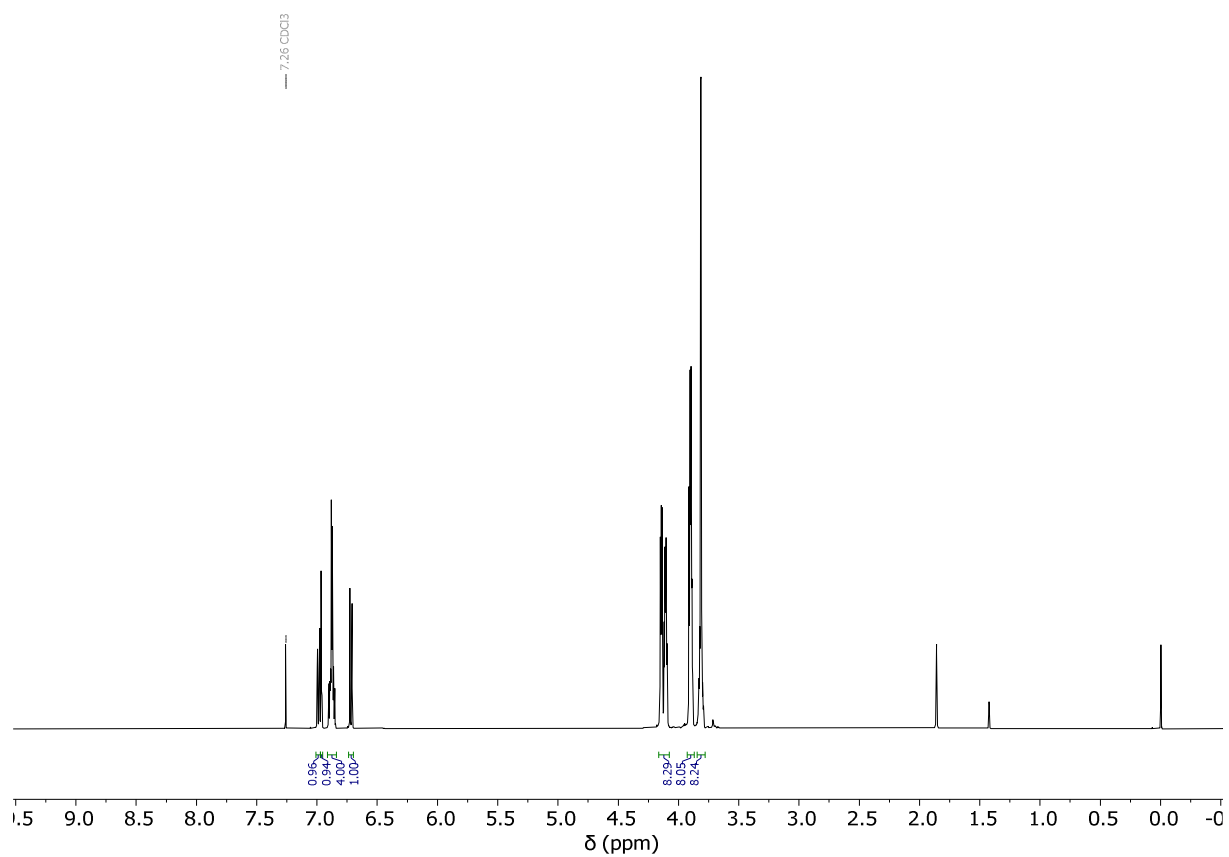


Figure 38. ^1H NMR spectrum of compound 7 (500 MHz, CDCl_3 , 298K)

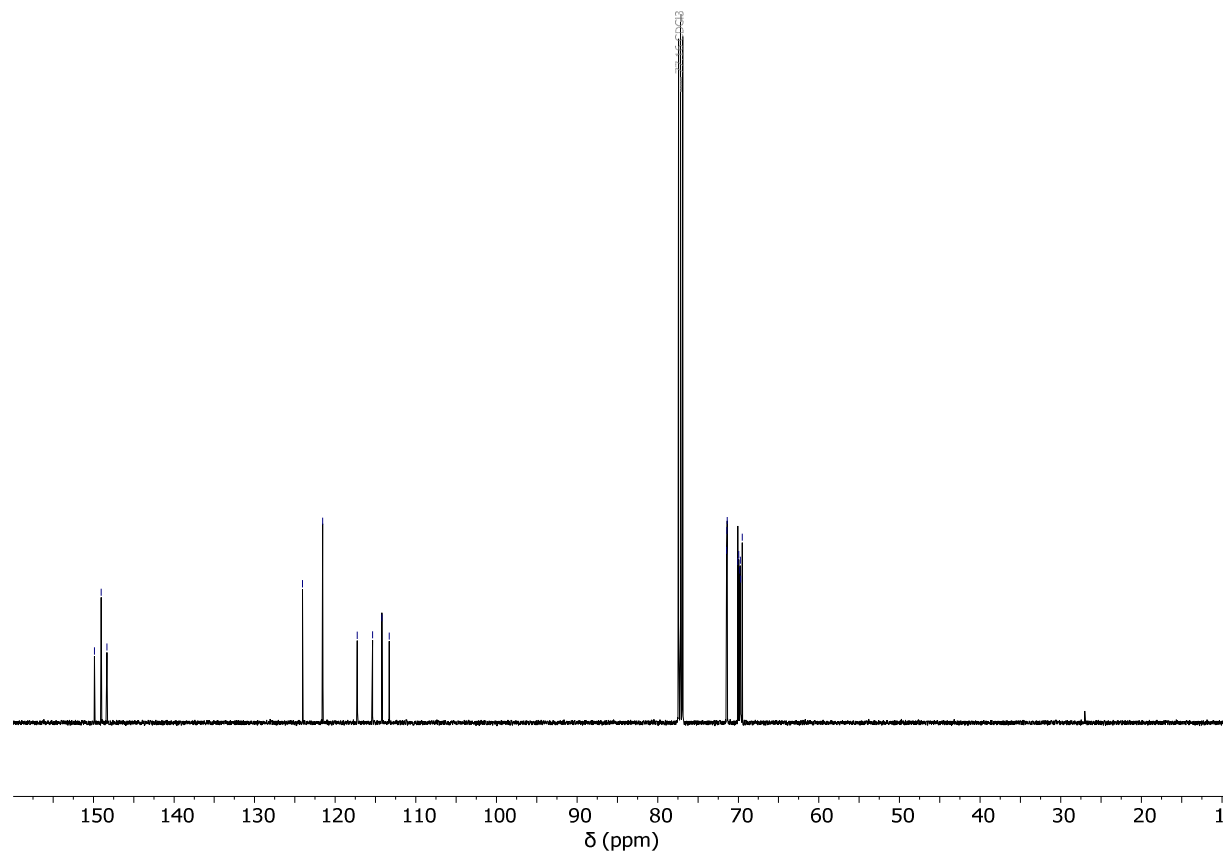


Figure 39. ^{13}C NMR spectrum of compound 7 (126 MHz, CDCl_3 , 298K)

^1H NMR and ^{13}C NMR spectra of compound A

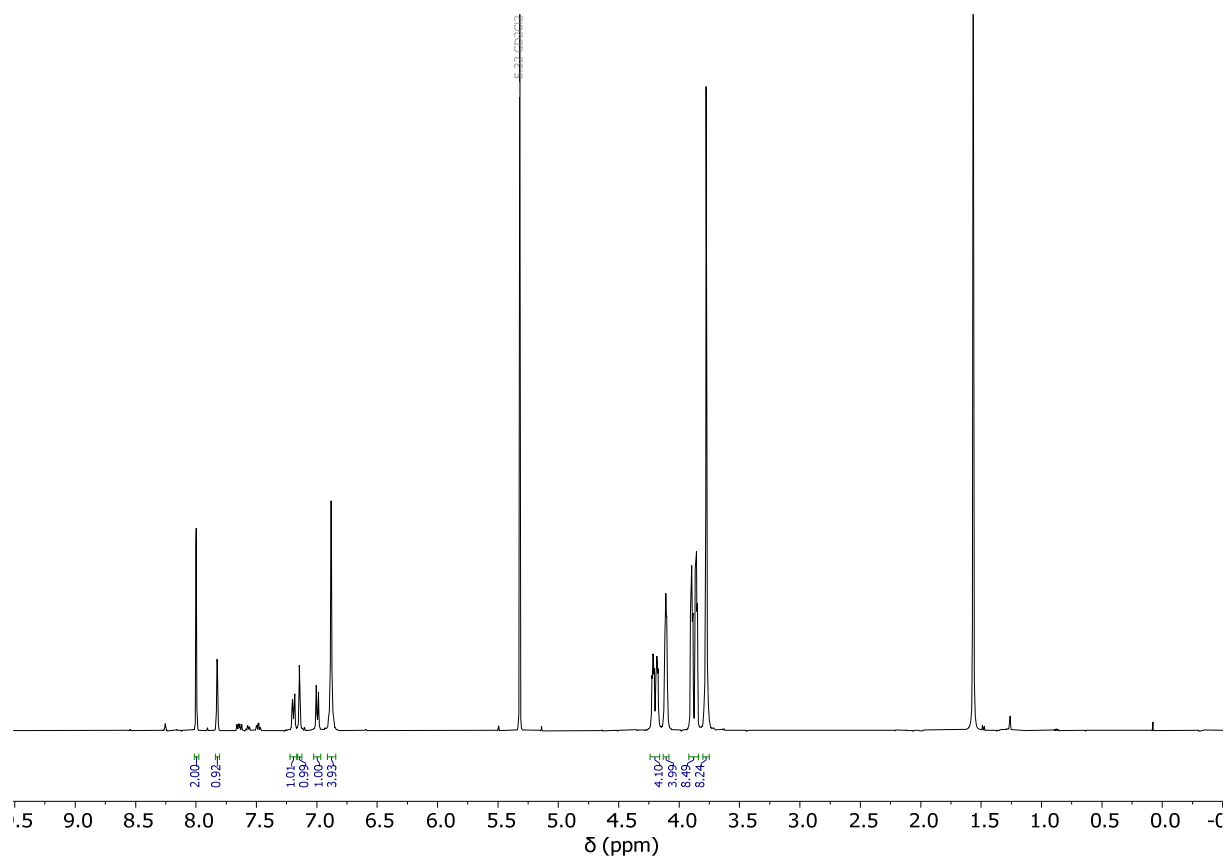


Figure 40. ^1H NMR spectrum of compound A (500 MHz, CD_2Cl_2 , 298K)

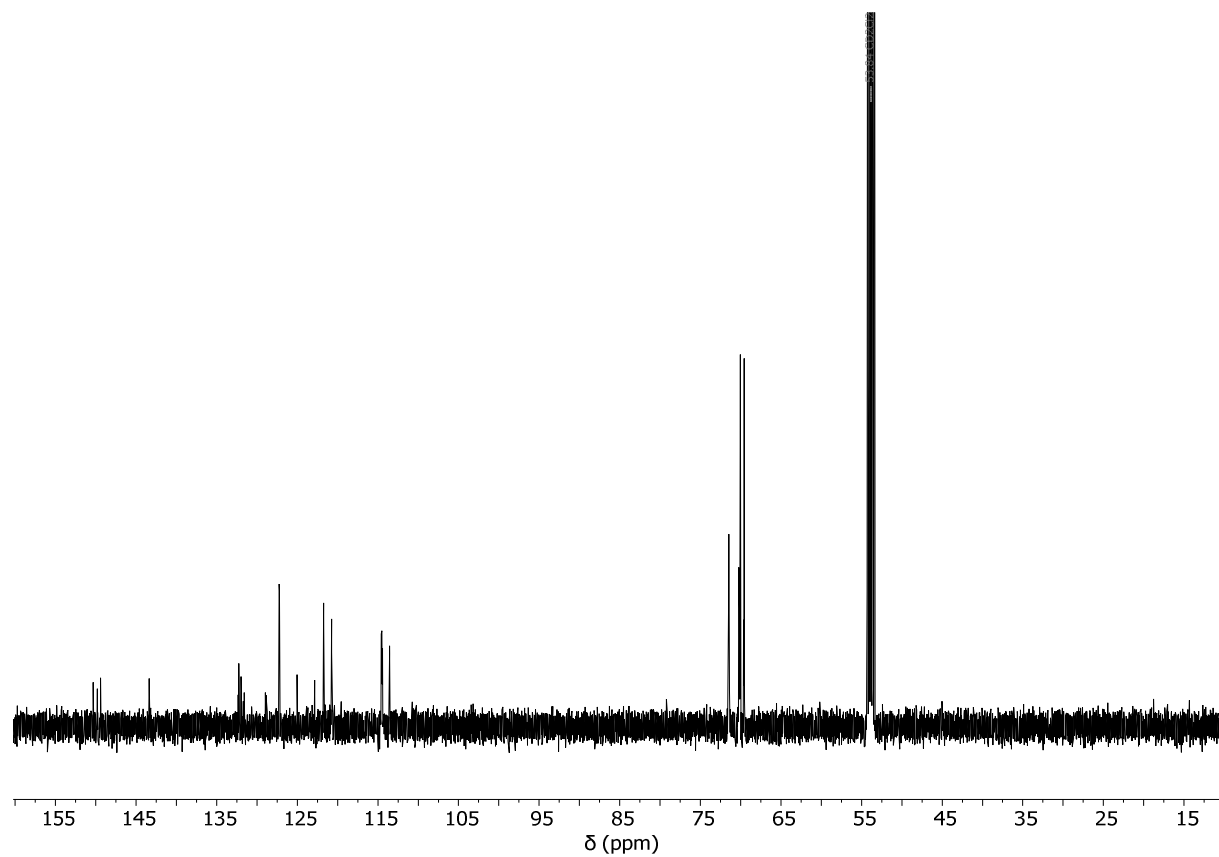


Figure 41. ^{13}C NMR spectrum of compound A (126 MHz, CD_2Cl_2 , 298K)

^1H NMR and ^{13}C NMR spectra of compound B

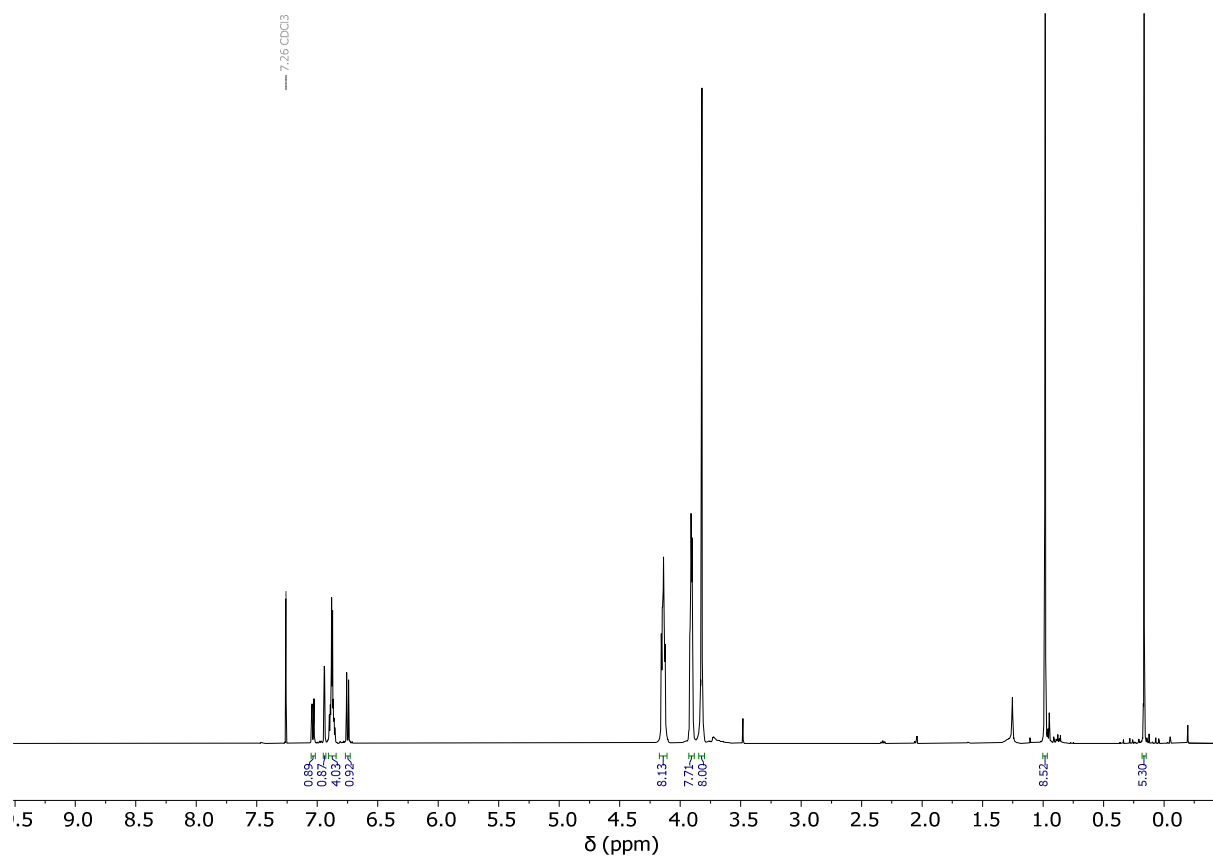


Figure 42. ^1H NMR spectrum of compound B (500 MHz, CDCl_3 , 298K)

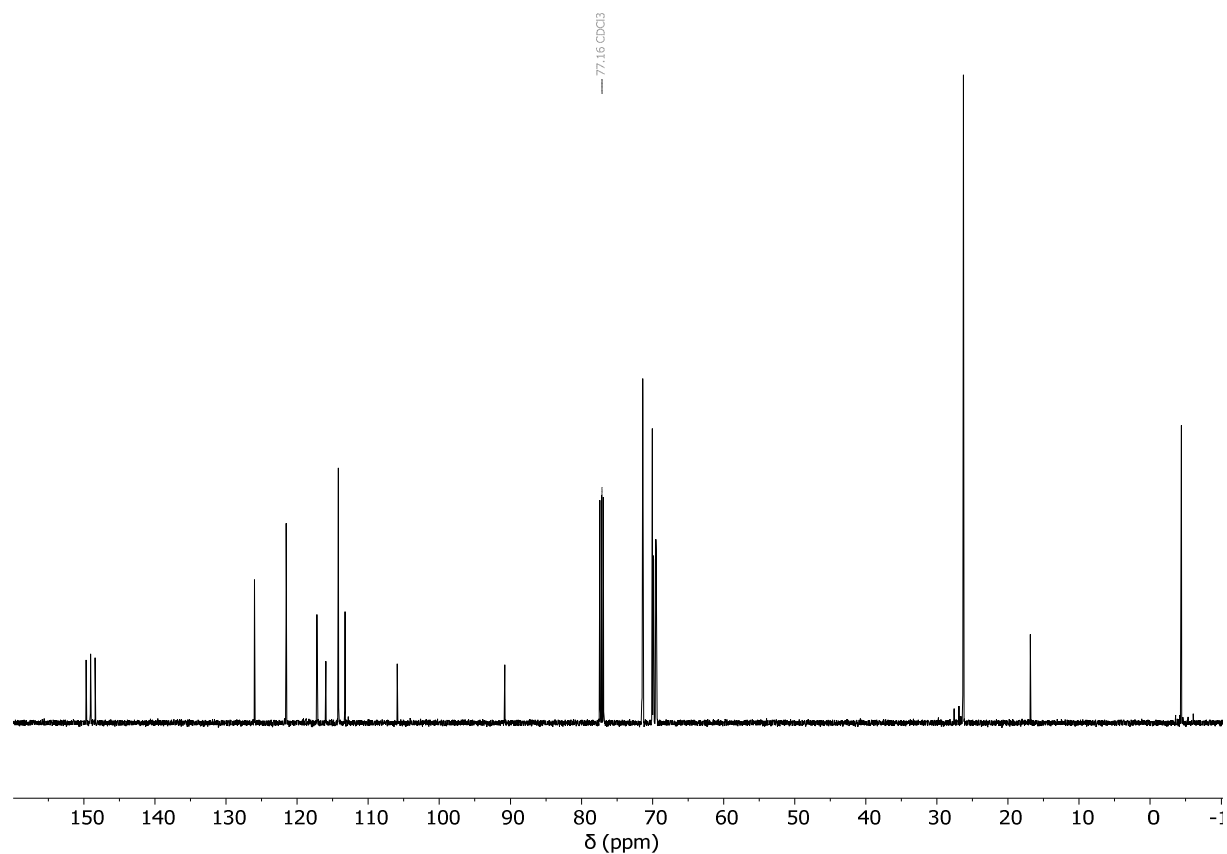


Figure 43. ^{13}C NMR spectrum of compound B (126 MHz, CDCl_3 , 298K)

^1H NMR and ^{13}C NMR spectra of compound $1a\text{H}^+$

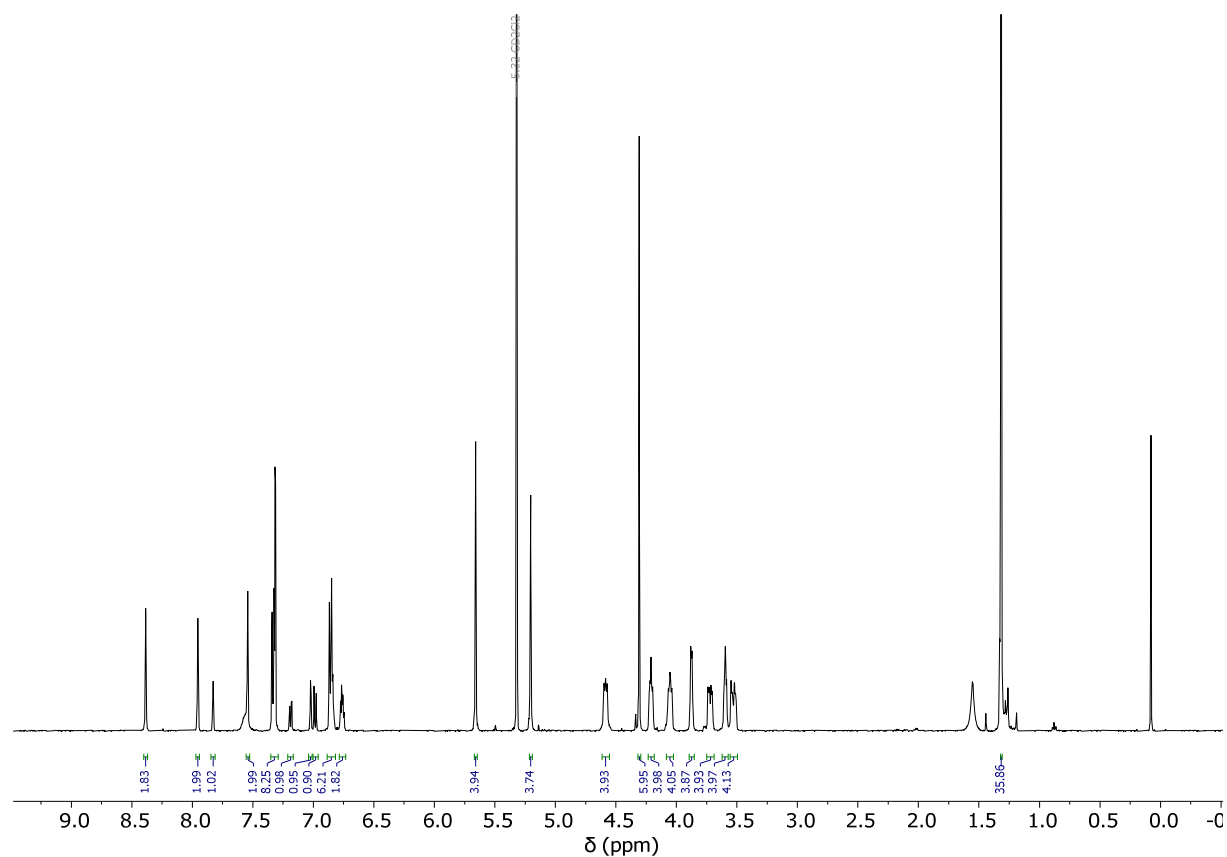


Figure 44. ^1H NMR spectrum of compound $1a\text{H}^+$ (500 MHz, CD_2Cl_2 , 298K)

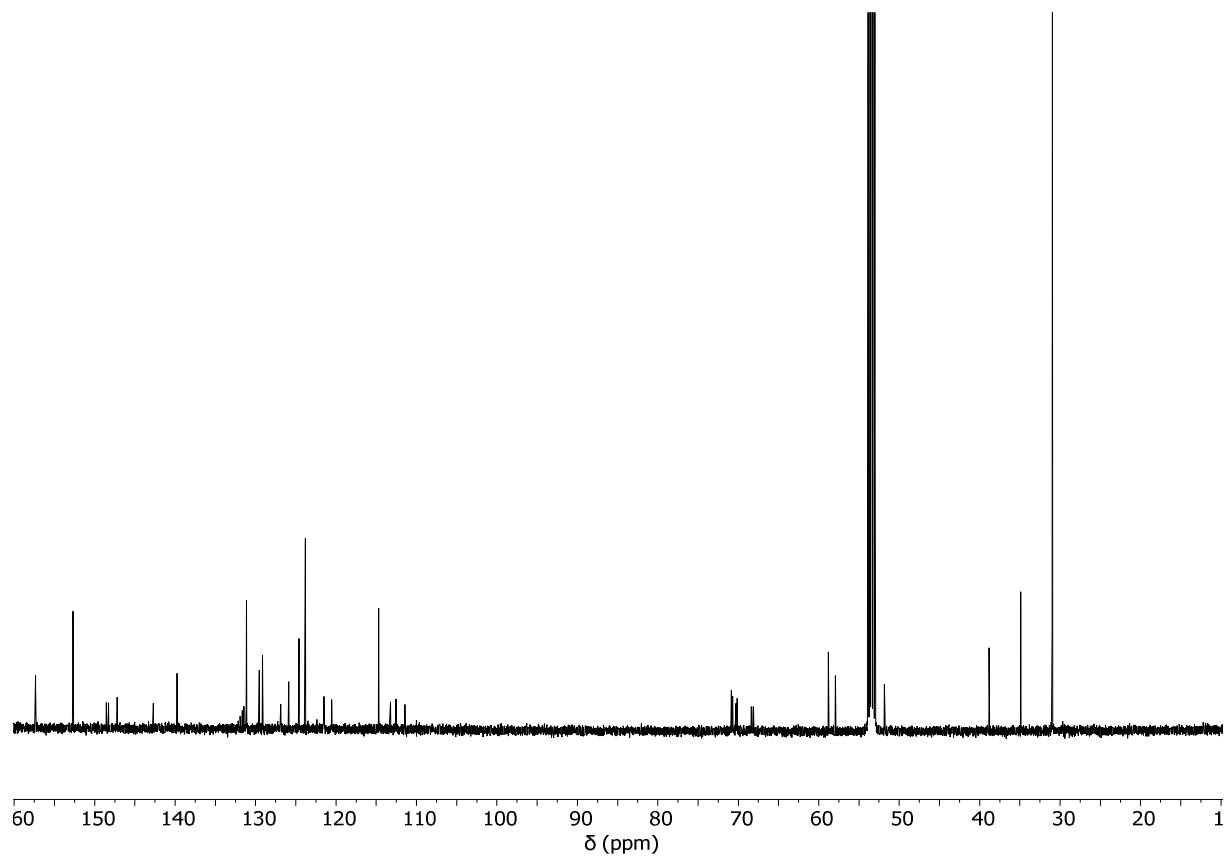


Figure 45. ^{13}C NMR spectrum of compound $1a\text{H}^+$ (126 MHz, CD_2Cl_2 , 298K)

^1H NMR and ^{13}C NMR spectra of compound $1b\text{H}^+$

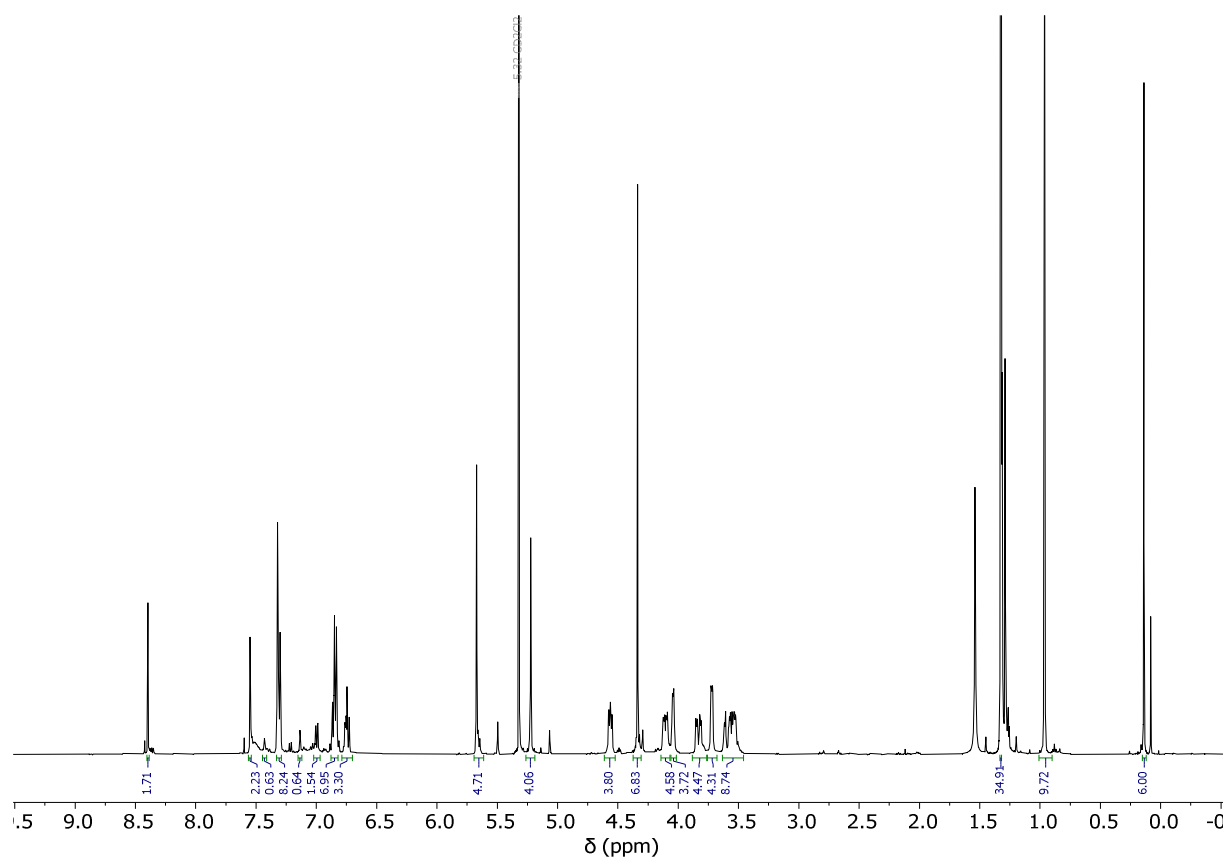


Figure 46. ^1H NMR spectrum of compound $1b\text{H}^+$ (500 MHz, CD_2Cl_2 , 298K)

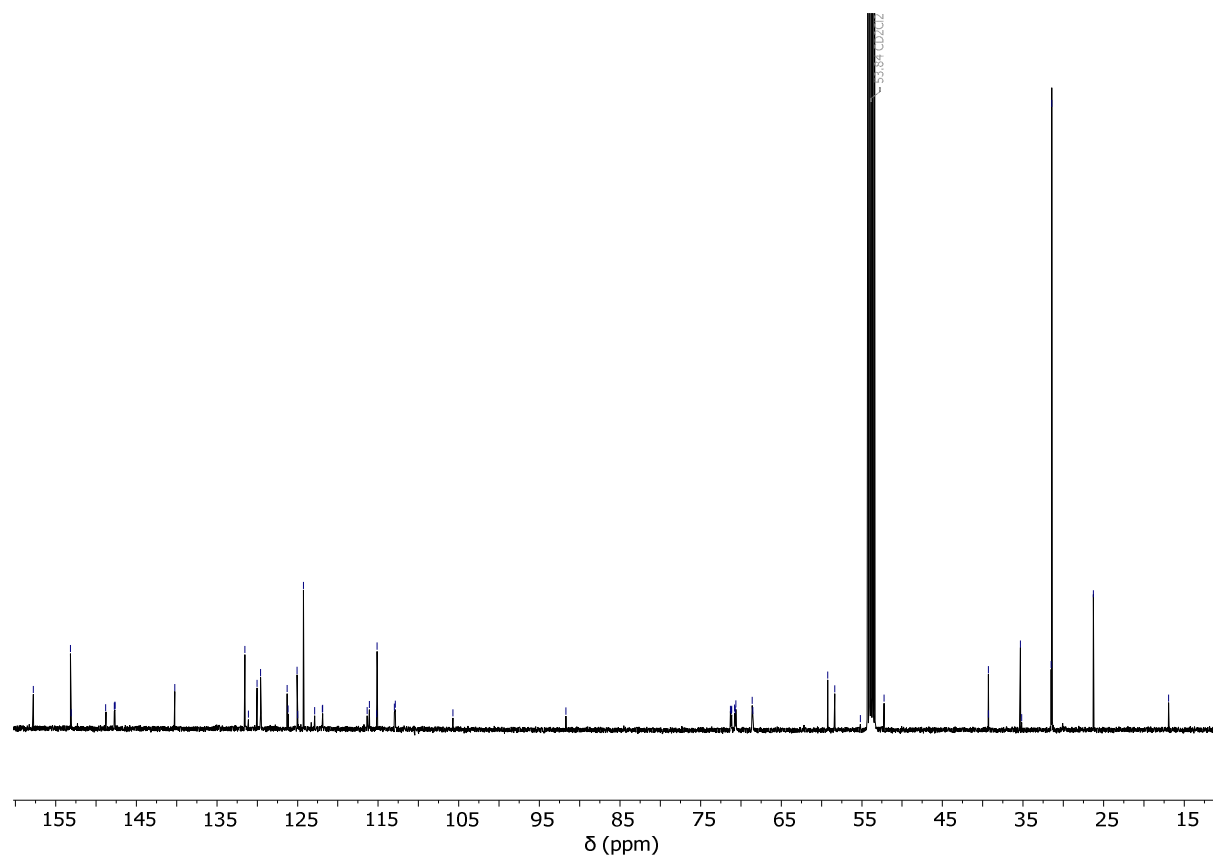


Figure 47. ^{13}C NMR spectrum of compound $1b\text{H}^+$ (126 MHz, CD_2Cl_2 , 298K)

6. REFERENCES

- ¹ J. F. Stoddart, *Angew. Chem. Int. Ed.* **2017**, *56*, 11094–11125.
- ² J. P. Sauvage, *Angew. Chem. Int. Ed.* **2017**, *56*, 11080–11093.
- ³ C. J. Bruns, J. F. Stoddart, *The Nature of the Mechanical Bond: from Molecules to Machines*, Wiley, **2017**.
- ⁴ H. L. Frisch, E. Wasserman, *J. Am. Chem. Soc.* **1961**, *83*, 3789–3795
- ⁵ J.-M. Lehn, A. Rigault, J. Siegel, J. Harrowfield, B. Chevrier, D. Moras, *Proc. Natl. Acad. Sci. U.S.A.* **1987**, *84*, 2565.
- ⁶ C. O. Dietrich-Buchecker, J. P. Sauvage, *J. Am. Chem. Soc.* **1984**, *106*, 3043–3045.
- ⁷ I. T. Harrison, *J. Chem. Soc. Chem. Comm.* **1972**, *2102*, 231–232.
- ⁸ J. D. Crowley, S. M. Goldup, A. Lee, D. A. Leigh, R. T. McBurney, *Chem. Soc. Rev.* **2009**, *38*, 1530–1541.
- ⁹ P. R. Ashton, E. J. T. Chrystal, P. T. Glink, S. Menzer, C. Schiavo, N. Spencer, J. F. Stoddart, P. A. Tasker, A. J. P. White, D. J. Williams, *Chem. Eur. J.* **1996**, *2*, 6.
- ¹⁰ T. Chang, A. M. Heiss, S. J. Cantrill, M. C. T. Fyfe, A. R. Pease, S. J. Rowan, J. F. Stoddart, A. J. P. White, D. J. Williams, *Org. Lett.* **2000**, *2*, 2947–2950.
- ¹¹ H.-Y. Zhou, Y. Han, C.-F. Chen, *Mater. Chem. Front.* **2020**, *4*, 12–28.
- ¹² F. Coutrot, E. Busseron, *Chem. Eur. J.* **2008**, *14*, 4784–4787.
- ¹³ M.-V. Martinez-Diaz, N. Spencer, J. F. Stoddart, *Angew. Chem. Int. Ed. Engl.* **1997**, *36*, 17.
- ¹⁴ V. Blanco, A. Carlone, K. D. Hänni, D. A. Leigh, B. Lewandowski, *Angew. Chem. Int. Ed.* **2012**, *51*, 5166–5169.
- ¹⁵ E. A. Neal, S. M. Goldup, *Chem. Commun.*, **2014**, *50*, 5128–5142.
- ¹⁶ A. C. Fahrenbach, C. J. Bruns, D. Cao, J. F. Stoddart, *Acc. Chem. Res.* **2012**, *45*, 1581–1592.
- ¹⁷ E. L. Eliel, S. H. Wilen, *Stereochemistry of organic compounds*. Wiley, **1994**.
- ¹⁸ K. Mislow, J. Siegel, *J. Am. Chem. Soc.* **1984**, *106*, 3319–3328.
- ¹⁹ P. Y. Bruice, *Essential organic chemistry*, Upper Saddle River: Pearson Education, **2006**.
- ²⁰ A. D. McNaught, A. Wilkinson, *IUPAC Compendium of Chemical Terminology*, 2nd ed.(the “Gold Book”), Blackwell Scientific Publications, **1997**.

-
- ²¹ B. Alberts, A. Johnson, J. Lewis, M. Raff, K. Roberts, P. Walters, *The Shape and Structure of Proteins. Molecular Biology of the Cell*, New York and London: Garland Science, Fourth Edition **2002**.
- ²² E. N. Jacobsen, A. Pfaltz, H. Yamamoto, *Comprehensive Asymmetric Catalysis*, Springer Berlin, **1999**.
- ²³ Nic M., Jirat J., Kosata B., “*Enantiomer excess*”, *IUPAC Compendium of Chemical Terminology*, **2006**.
- ²⁴ S. Corra, C. de Vet, J. Groppi, M. La Rosa, S. Silvi, M. Baroncini, A. Credi, *J. Am. Chem. Soc.* **2019**, *141*, 9129–9133.
- ²⁵ E. M. G. Jamieson, F. Modicom, S. M. Goldup, *Chem. Soc. Rev.* **2018**, *47*, 5266–5311.
- ²⁶ M. A. Jinks, A. de Juan, M. Denis, C. J. Fletcher, M. Galli, E. M. G. Jamieson, F. Modicom, Z. Zhang, S. M. Goldup, *Angew. Chem. Int. Ed.* **2018**, *57*, 14806–14810.
- ²⁷ C. Yamamoto, Y. Okamoto, T. Schmidt, R. Jäger, F. Vögtle, *J. Am. Chem. Soc.* **1997**, *119*, 10547–10548.
- ²⁸ H. B. Kagan, J. C. Fiaud, *Topics in stereochemistry*, Wiley, **1988**, *18*, 249–330.
- ²⁹ A. Imayoshi, B. V. Lakshmi, Y. Ueda, T. Yoshimura, A. Matayoshi, T. Furuta, T. Kawabata, *Nat. Commun.* **2021**, *12*, 404.
- ³⁰ E.V. Anslyn, D. Dougherty, *Modern physical organic chemistry*, University science books, **2006**.
- ³¹ C. J. Pedersen, *J. Am. Chem. Soc.* **1967**, *89*, 2495–2496.
- ³² D. Maciejewska, J. Jakowski, J. Kleps, G. Chałasinski, *J. Mol. Struct.* **2004**, *680*, 5–13.
- ³³ W.E. Stewart, T.H. Siddall, *Chem. Rev.* **1970**, *70*, 517–551.
- ³⁴ S. Corra, C. de Vet, M. Baroncini, A. Credi, S. Silvi, *Chem.* **2021**, *7*, 2137–2150.